A ONE-DIMENSIONAL FOURIER ANALOGUE COMPUTER

AND ITS APPLICATION TO THE REFINEMENT OF THE

STRUCTURE OF CUBANITE

by

LEONID V. AZAROFF

B.S., Tufts College
(1948)

SUBMITTED IN PARTIAL FULFILLMENT OF THE

REQUIREMENTS FOR THE DEGREE OF

DOCTOR OF PHILOSOPHY

at the

MASSACHUSETTS INSTITUTE OF TECHNOLOGY

(1953)

Signature of Author. . . . .
        Department of Geology and Geophysics, October 1, 1953

Certified by . . . .
                                    Thesis Supervisor

Accepted by . . . .
        Chairman, Departmental Committee on Graduate Students

A ONE-DIMENSIONAL FOURIER ANALOGUE COMPUTER

AND ITS APPLICATION TO THE REFINEMENT OF THE

STRUCTURE OF CUBANITE

LEONID V. AZAROFF

Submitted to the Department of Geology on October 1, 1953

in partial fulfillment of the requirements for the degree

of Doctor of Philosophy.

A computer has been constructed to sum Fourier series having up to 30 terms. Although this is a one-dimensional computer, it can be used for double and triple summations by using standard trigonometric expansions. Secondarily, it can be used for computing trial structure factors.

O.D.F.A.C. sums $\sum_{n} F_n \frac{\sin}{\cos} 2\pi n x$ electrically. The trigonometric function is produced by a variable-angle transformer known as a resolver. Each amplitude is set by a variac which regulates the input to a particular resolver. The frequencies $2\pi n x$ for 31 values of n are arranged by gearing the rotors of the resolvers in ratios 0, 1, 2, . . . 30. The resultant individual currents are added in parallel and the value at point x (in intervals of $\frac{1}{60}$, $\frac{1}{120}$, or $\frac{1}{240}$ of a cell edge) is read on a voltmeter and the phase is read on an oscilloscope.

The relative speed of a computation is five to ten times faster than the standard strip method. The average error in a computation compares favorably with the rounding off error in conventional two-place strips.

This computer has been utilized in the refinement of the structure of cubanite. The original structure determined by M. J. Buerger has been confirmed. The space group is Pcmn with $a = 6.46_3$A, $b = 11.117$ A, $c = 6.233$ A.

The intensities used in the refinement procedure were corrected for Lorentz and polarization factors and for absorption by the crystal. The refinement was carried

out by successive Fourier approximations. First, the a
and c axis projections were refined, followed by the re-
finement of two plane sections. The final stage of re-
finement was carried out by passing three, mutually-per-
pendicular line sections through each atom. Difference
electron densities were also computed for these line
sections yielding the final atomic coordinates. The
final atomic coordinates are listed and the bond lengths
and bond angles are discussed.

Thesis Supervisor: Martin J. Buerger

Title: Professor of Minerology and Crystallography

TABLE OF CONTENTS

LIST OF ILLUSTRATIONS

TABLE INDEX

INTRODUCTION

The work described in this thesis comprises two distinct problems. The first part deals with the design and construction of a one-dimensional analogue computer for performing Fourier series summations. Fourier series are continuously utilized in such crystallographic problems as structure determination, structure refinement and others. Although this computer was designed for express use in the crystallography laboratory, its application is more universal, since Fourier series are used in solving different problems in all fields of science.

The second part of this thesis describes the procedure of refining the structure of cubanite. Since the computer described in Part I was used extensively in this refinement procedure, Part II forms a logical sequel.

Part I. A One-Dimensional Fourier Analogue Computer

Introduction

Earlier computers. Fourier series are important
in many branches of science. One-dimensional, two-dimen-
sional, and three-dimensional Fourier series are especially
important in x-ray crystallography. Since the computation
of these functions is tedious, a number of devices have
been developed to perform the computation, only a few of
which have come into common use. Among these are the
electrical digital devices of Beevers[1,2], the electrical
analogue machines of Hägg and Laurent[3], Ramsay, et al[4],
the mechanical analogue devices of McLachlan and Champaygne[5],
Rose[6], Vand[7] and Beevers and Robertson[8]. All these devices
sum one-dimensional series. Robertson[9], Pepinsky[10,11],
and McLachlan et al[12] have devised electrical analogue
machines for two-dimensional Fourier summations.

Basis for design. When the number of Fourier
syntheses to be computed in the Crystallographic Laboratory
of M.I.T. became large enough to warrant using a special
computing device, several of these machines were closely
investigated. Some were found to have obvious defects,
such as contact trouble when multiple telephone switches
were used. Most of them were found to handle too limited
a number of Fourier terms. Guided by this survey, a
decision was reached to build a one-dimensional electri-
cal analogue computer which would sum a comparatively

large number of Fourier terms. This was specifically set at 30, since this is about as high as ever required in the analysis of ordinary non-protein crystal structures. McLachlan's computer[12] served as a guide and as a point of departure. His machine compounds phases electrically by using selsyns. It performs a two-dimensional synthesis but is limited to 8 x 8 terms.

The transformation of an angle, φ, into a trigonometric function can be performed electrically in many different ways. The two devices considered in the early stages of designing ODFAC were sine potentiometers and resolvers. A sine potentiometer consists of a continuous resistor winding tapped to produce a voltage which varies as the sine of the angle of rotation of the main shaft. A resolver is a transformer using as its primary the rotor member and as its secondary two separate stator windings placed 90 degrees apart. When a voltage is applied to the primary winding the voltages of the two secondary windings vary respectively as the sine and cosine of the angle of rotation. Resolvers were chosen for the construction of ODFAC because the isolating property of a transformer makes the adding circuit independent of variations in the input stages.

Principle of operation. Fig. 1 shows, in outline form, the operation of ODFAC. The input to each resolver, R, is fed from a variac, V. The variac thus controls the

amplitude or Fourier coefficient, $\underline{A}$, of the Fourier component of a particular resolver. The two outlet leads of the resolver then deliver voltages proportional to $\underline{A}$ $\cos \Upsilon$ and $\underline{A}$ $\sin \Upsilon$. The shafts of 30 such resolvers are geared so that the shaft displacement of a particular resolver, $\underline{n}$, is an integral multiple, $\underline{n}$, of the shaft displacement of a fundamental shaft. The outputs of the individual resolvers are therefore a set of voltages proportional to

$$A_0$$
$$A_1 \cos \Upsilon_1 \qquad\qquad A_1 \sin \Upsilon_1$$
$$A_2 \cos \Upsilon_2 \qquad\qquad A_2 \sin \Upsilon_2$$
$$\bullet \qquad\qquad\qquad \bullet$$
$$\bullet \qquad\qquad\qquad \bullet$$
$$A_{30} \cos \Upsilon_{30} \qquad\qquad A_{30} \sin \Upsilon_{30}$$

if the outputs are appropriately coupled, the machine produces voltages proportional to

$$\sum_{n=0}^{30} A_n \cos \Upsilon_n \quad \text{and} \quad \sum_{n=0}^{30} A_n \sin \Upsilon_n$$

which can be read on a voltmeter, $\underline{VM}$. In crystallographic problems $\Upsilon_n = 2\pi n\underline{x}$ where $\underline{n}$ is the number of the harmonic and $\underline{x}$ is the sampling interval expressed as a fraction of one complete period.
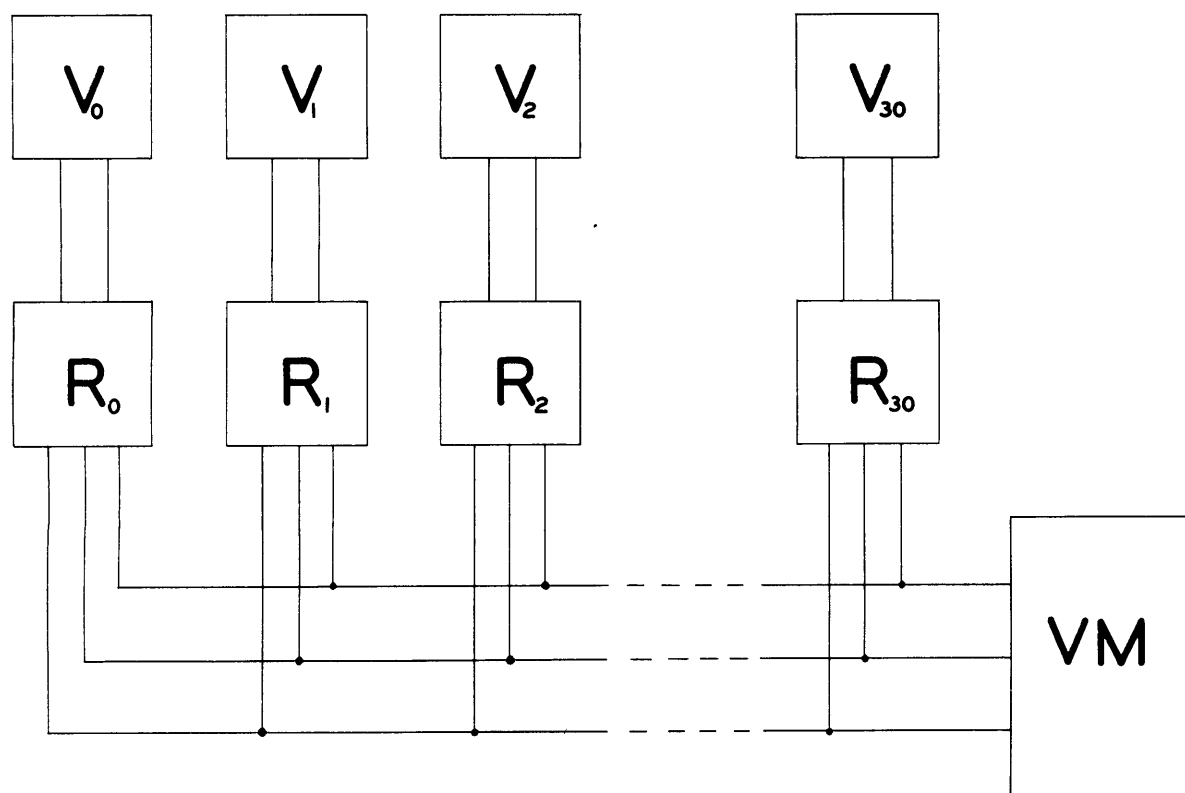
Fig. 1   ODFAC Outline

Design and construction

Mechanical features. The production of thirty harmonics in the Fourier series requires that one complete rotation of the rotor in the first resolver corresponds to two complete rotations of the rotor in the second resolver, etc., up to thirty complete rotations of the rotor in the thirtieth resolver. This is accomplished in ODFAC by means of a gear train represented by Fig. 2.

The main shaft leading from the motor is geared by worms and worm gears to three horizontal shafts whose relative angles of rotation are given by the ratios of the worms and gears. Each horizontal shaft carries a series of spur gears which engage with the spur gears mounted on the rotors of the individual resolvers. The angle of rotation of each rotor shaft is, therefore, a function of the ratio of its spur gears modified by the angular rotation of the horizontal shafts. The actual gear train is shown in Fig. 3. This particular gear train has several advantages. One is that most gears used are commercially available, stock sizes. Only 10 of the 82 gears are nonstandard size and had to be obtained by special order. Another advantage is that high gear ratios are avoided, the largest step-down ratio being 5:4. This decreases inaccuracies in the positioning of the resolver shafts.

Because of low frictional losses, all 30 resolvers can be driven at the desired speed by a small, $\frac{1}{1500}$ h.p. motor.

	1	2	3	4	5	6	7	8	9	10
	144	144	144	96	96	96	96	72	96	96
1 | 60	18	36	54	48	60	72	84	72	108	120
	1:8	2:8	3:8	4:8	5:8	6:8	7:8	8:8	9:8	10:8

	11	12	13	14	15	16	17	18	19	20
	96	96	96	96	96	72	96	96	96	96
1 | 30	66	72	78	84	90	72	102	108	114	120
	11:16	12:16	13:16	14:16	15:16	16:16	17:16	18:16	19:16	20:16

	21	22	23	24	25	26	27	28	29	30
	96	72	96	72	96	72	96	72	96	96
1 | 20	84	66	92	72	100	78	108	84	116	120
	21:24	22:24	23:24	24:24	25:24	26:24	27:24	28:24	29:24	30:24

Motor

Fig. 2 Gear Train

Fig. 3   Gear Train

Electrical circuit. The wiring diagram of the electrical components of ODFAC is shown in Fig. 4. The input voltage is fed from the variacs, $\underline{V}$, through a DPDT phase-selector switch, $\underline{S}$, to the rotors of the resolvers, $\underline{R}$, which are linked by the gear train illustrated in Fig. 3. Each output line of the stator winding of the resolvers contains a series resistance,$\underline{r}$,of 500,000 ohms whose purpose is to make any stray losses in the secondary circuit negligible. All the cosine (and sine) windings of even harmonics are connected in parallel. Similarly the cosine (and sine) windings of the odd harmonics are connected in parallel. These lines lead to a gang switch which permits various combinations of the lines to be made.

The use of a parallel, rather than a series adding circuit is preferred for the following reasons: In a series circuit all the stator windings would be directly connected causing a cumulation of errors due to mutual inductance between the individual primary and secondary windings and the secondary windings of adjacent resolvers. The addition of voltages in a series circuit would also have the disadvantage of building up very high voltages and currents with possible damage to the windings. All of these disadvantages are overcome by a parallel circuit in which the isolation of the individual resolvers limits the current in each secondary winding to that induced by the primary.
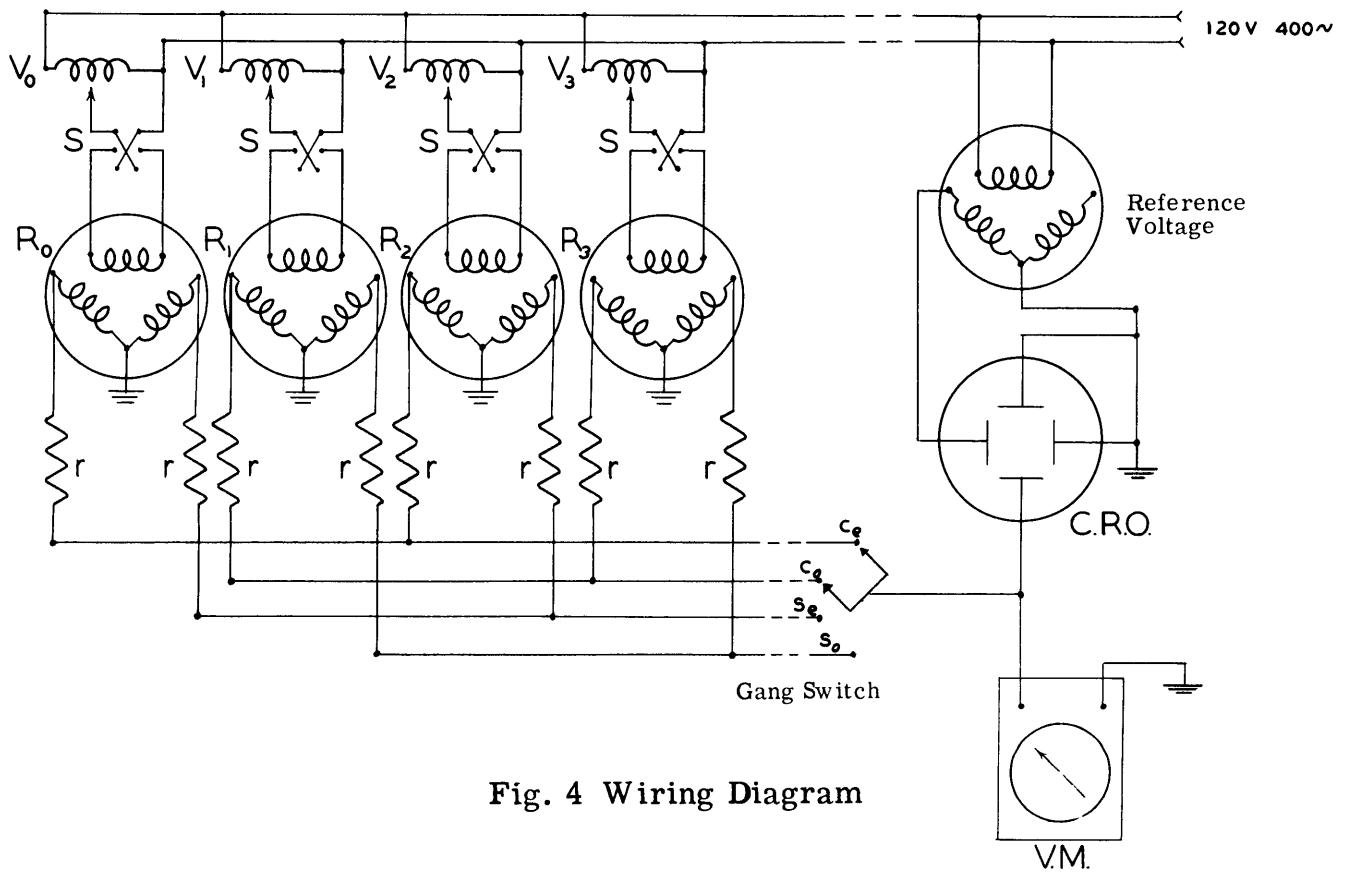
Fig. 4 Wiring Diagram

This isolation permits the insertion of a large resistance to minimize losses in the line. The maximum output voltage obtained from such a circuit can never exceed the input line voltage because the individual voltages are averaged over all 31 branches.

The output voltage lines pass through a 4-gang switch which selects combinations of odd and even harmonics of the sine or cosine lines for transmission to the voltmeter or oscilloscope. In practice, there are four such lines, viz. the lines for cosine even, cosine odd, sine even and sine odd. Each line is connected to appropriate terminals of the gangs. Thus, when the switch is rotated to a given position, it makes contact with only those leads that are connected at that position. The combinations presently available are: $\underline{\cos_e}$, $\underline{\cos_o}$, $\underline{\sin_e}$, $\underline{\sin_o}$, $\underline{\cos_e}$ + $\underline{\cos_o}$, $\underline{\sin_e}$ + $\underline{\sin_o}$, $\underline{\cos_e}$ + $\underline{\sin_o}$, and $\underline{\cos_o}$ + $\underline{\sin_e}$. The separation of the odd and even harmonics into separate lines permits the utilization of the symmetry inherent in sine and cosine functions. This is standard practice in crystallographic applications[13].

The meter has a 50 μa movement and three ranges which correspond to the voltages expected from the number of variacs supplying input voltages. A fourth range, actuated by a push-button, permits a clear reading of low voltages. The actual meter circuit is illustrated in Fig. 5.

The cathode-ray tube is part of a standard oscilloscope circuit not having a sweep generator. The circuit is illustrated in Fig. 6. The output voltage is placed across two deflecting plates and a reference voltage across the other two. Since both sets of plates have the same frequency applied to them, the resulting Lissajous figure on the tube face is a straight line whose angular inclination depends on the magnitude and relative phase of the output voltage.

Construction details. The rear view of the assembled machine is shown in Fig. 7. The resolvers are held in place by aluminum clamps (see also Fig. 3) which, in turn, are fastened to two aluminum angles forming a tack-like shelf. Each shelf holds five resolvers and supports its horizontal drive shaft mounted in ball-bearing supports. The clamps have built-in means for adjusting the angular position of the resolvers, consisting of a slot to accept a gear-bearing key which engages with the gear on the resolver body, permitting minor variations in angular alignement after the resolver has been positioned. The horizontal drive shafts are driven by the main drive shaft which runs vertically, in the center of Fig. 7, from the motor (hidden by the bottom shelf) to the control mechanism.

The control mechanism is connected directly to the drive shaft by a set of change gears. It consists of

100v

200v

20v

Ground

10v

METER
(rear view)

31

21

16

OFF

RANGE SELECTOR SWITCH

PUSH-BUTTON, SPDT

110v 60~
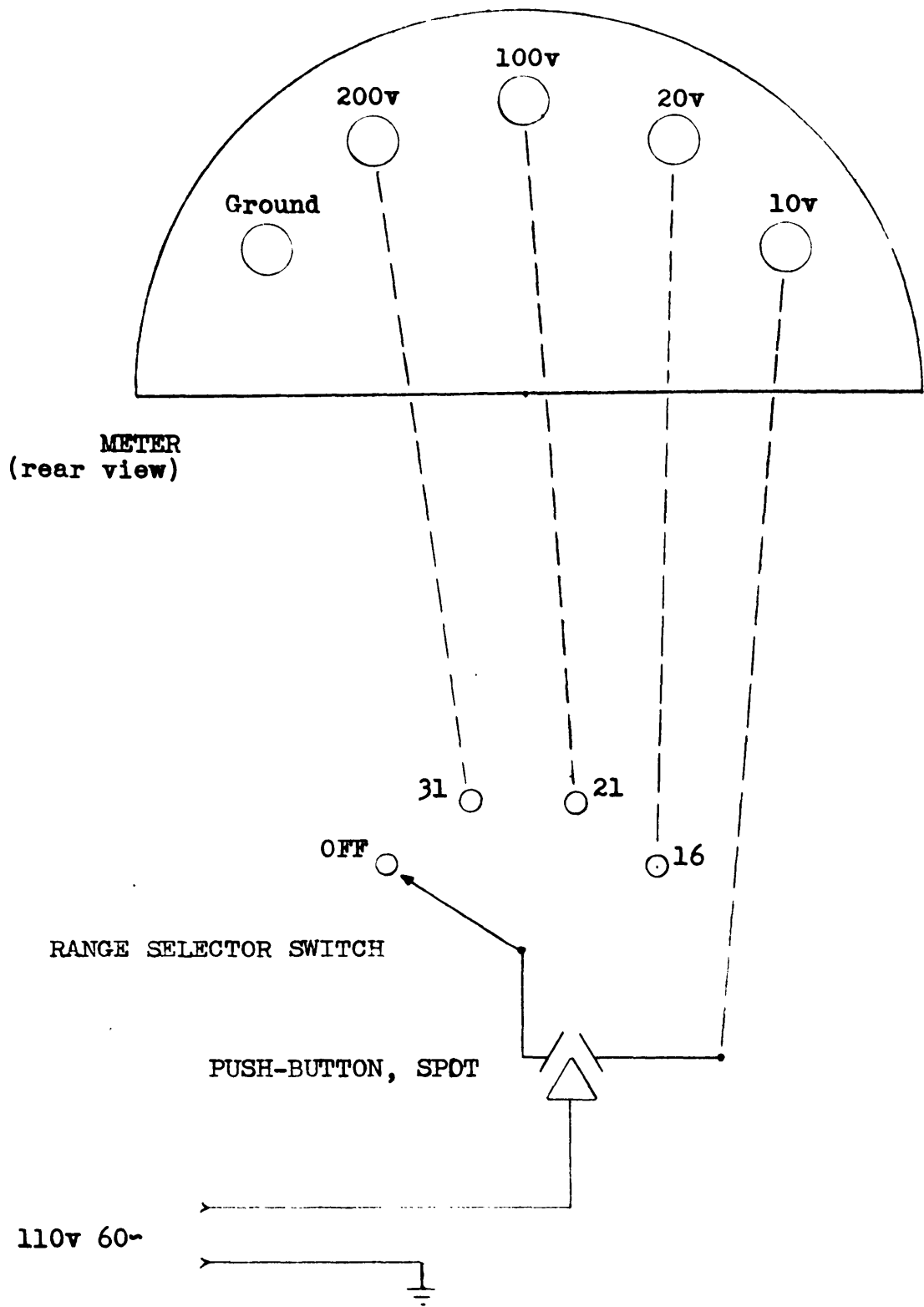
Fig. 5   Meter Circuit

Fig. 6 Oscilloscope Circuit

Fig. 6 Oscilloscope Circuit

LEGEND

P_1	3.0M potentiometer (Horizontal centering)
P_2	3.0M potentiometer (Vertical centering)
P_3	2.0M poténtiometer (Vertical gain control)
P_4	0.5M potentiometer (Horizontal gain control)
P_5	250K potentiometer (Focus control)
P_6	250K potentiometer (Intensity control)
r_1, r_2	82K 1 w
r_4, r_5	1.0M 1 w
r_6	1.2M 1 w
r_7	470K 1 w
r_8	2.2K 1 w
r_9	750K 1 w
r_{10}	100K 1 w
r_{11}	270K 1 w
r_{12}	70K 1 w
r_{13}	250K 1 w
c_1, c_2	.005 μf 1000 v
c_3, c_4	.002 μf 1000 v
c_5	.05 μf 400 v
c_6	10 μf 25 v
c_7	.4 μf 1000 v
c_8	8 μf 450 v
T_1	Power transformer (Chicago, PCC-60)
T_2	Filter choke (UTC, CG-45)
S	Selenium rectifiers (6, Federal, FTR 1159)

Control Mechanism

Resistor
Banks

C.R.O.

Motor

Motor-Generator

Reference
Voltage
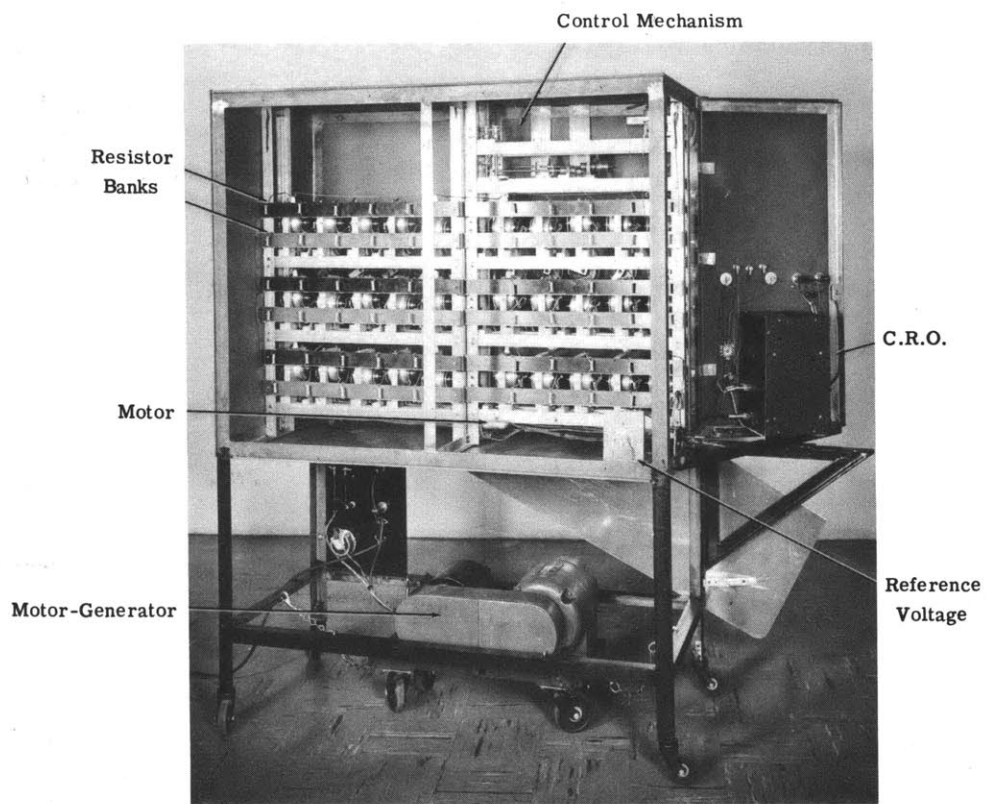
Fig. 7 ODFAC, Rear View

a shaft which carries a change gear and a cam. The cam
actuates a micro-switch which controls the number of
revolutions made by the motor for the sampling interval.
The motor is a dynamic-braking motor which can be stopped
instantaneously by applying a reverse field to its rotor.
The actual control circuit is illustrated in Fig. 8. A
horizontal shaft, permanently geared to the main drive
shaft, rotates a dial on the front panel indicating the
angular position of the main shaft. The change gears in
the control mechanism permit the selection of intervals
of $\frac{1}{60}$, $\frac{1}{120}$, or $\frac{1}{240}$ of one complete period.

The motor-generator set at the bottom of Fig. 7
provides the input voltage (120 v., 400~) to the variacs
only. The driving mechanism and service components operate
on the regular line voltage. The purpose of the motor-
generator set is to provide a constant current source
with an undistorted wave shape, making the adding circuits
in ODFAC independent of line fluctuations.

CAM

MICRO-SWITCH

TOGGLE SWITCH
SPST

PUSH BUTTON
SPST Norm. Closed

MOTOR

110v 60~
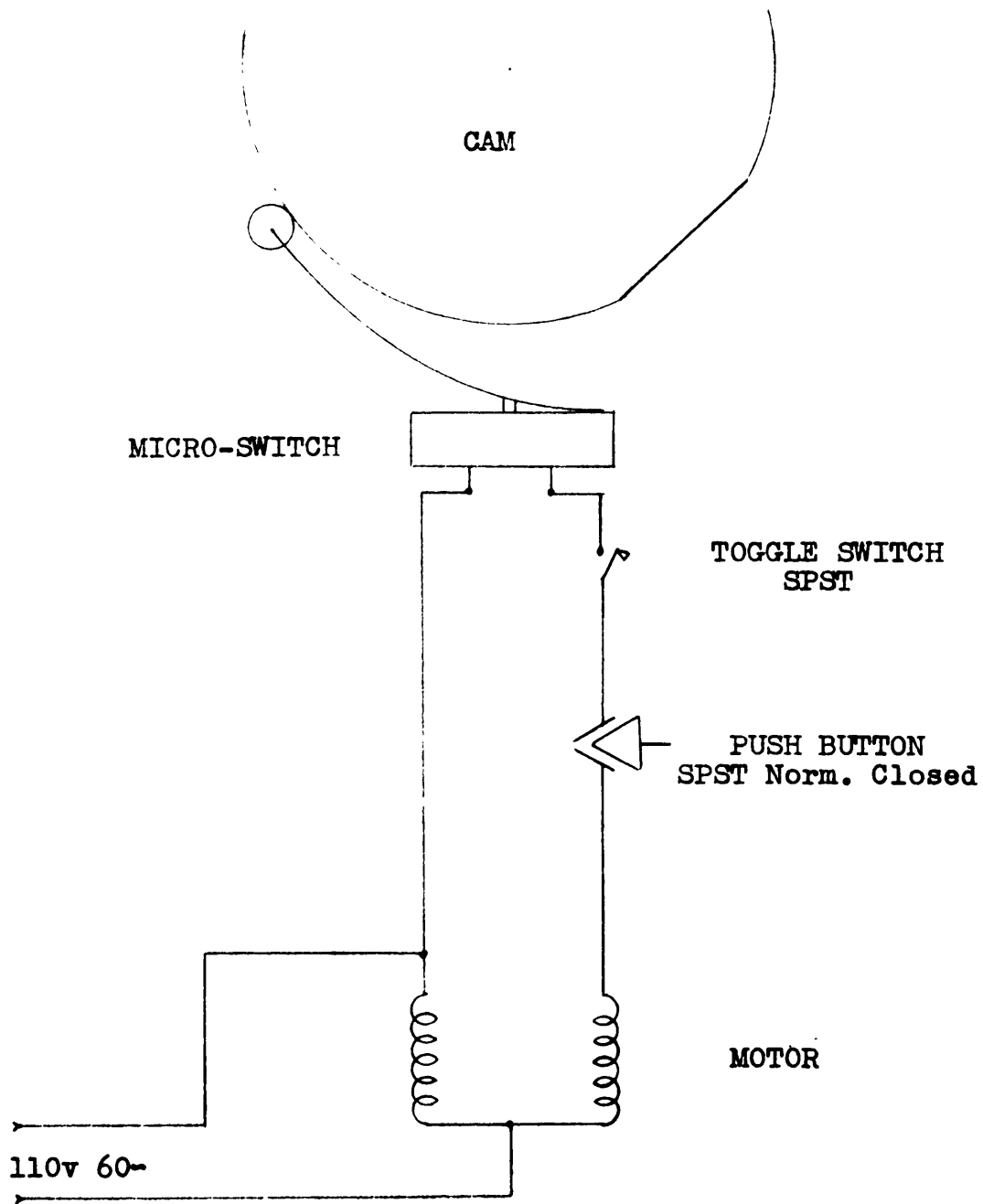
Fig. 8   Control Circuit

Performance

Operation. A front view of ODFAC in operation is shown in Fig. 9. The variacs are numbered and arranged on removable panels in sets of five. The amplitudes are set by means of a friction-drive dial permitting an accurate, rapid setting from 0-100. The phases are set by means of a plus-minus toggle switch placed directly above each dial. Each bank of five resolvers can be switched in or out of the input curcuit by means of an additional toggle switch on the left of each panel. The numbering and location of the dials is such that the operator sits facing the first sixteen dials, the next fifteen dials being within arm's-length to his right. The dials need be set only once for each one-dimensional summation.

A panel to the left of the operator contains the meter on which the value of the Fourier series is read, the CRO tube on which the positive and negative quadrants are marked, the sine-cosine selector switch, and a push-button that advances the computer mechanism to the next sample setting. A pilot light indicates that the motor has advanced the computer to the next sample setting and the meter may be read. Once the amplitudes (variac dials) and the phases (plus-minus switches) have been set, and
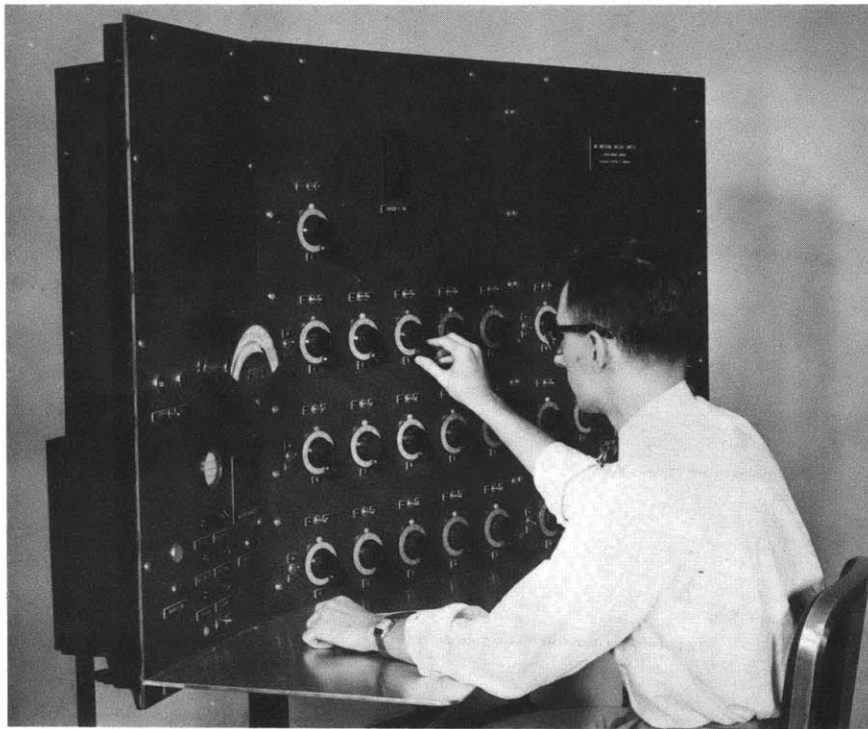
Fig. 9 ODFAC, Front View

the type series (sine or cosine) has been selected, all
the operator does is read the meter, note the phase, and
push the button to advance to the next reading. A drop-
leaf table is attached to the front of ODFAC to provide a
convenient surface for recording readings.

The speed of a computation on ODFAC depends
primarily on the type of series desired, i.e., one-
dimensional, two-dimensional, etc., and only secondarily
on the number of terms or frequency of interval of sampling
desired. The machine time for a complete cycle from 0 to
2π has been selected to take 7 minutes. If the time for
setting the variacs and recording the values obtained is
added to this, the total computing time amounts to approxi-
mately 10-15 minutes, depending on the sampling interval
selected. The relative time of computing an average two-
dimensional series on ODFAC ranges from $\frac{1}{5}$ to $\frac{1}{10}$ of the time
consumed using standard strip methods[14],[15]. The more terms
there are in the series and the finer the interval of
sampling desired, the more efficient ODFAC becomes when
compared with strip methods.

Accuracy. The accuracy of the components used
in ODFAC is the highest attainable at a reasonable cost.
The resolvers are accurate to within $1\frac{1}{2}$ mechanical degrees.
The variacs and resistors are accurate to within 1% of
maximum ratings. The meter is accurate to better than

1% of full scale deflection. The backlash in the gears
is almost non-existent and the angular accuracy of the
gear settings is within a fraction of one degree.

Table 1 shows an actual comparison of the meter
readings of ODFAC with those computed using three-place
trigonometric tables. The amplitudes for this one-
dimensional series were supplied by Professor M. J. Buerger
from a Harker line synthesis for realgar. In the same
table are listed corresponding values as computed with
the aid of Patterson-Tunell strips[14] and Beevers-Lipson
strips[15]. If the deviations from the true values are
examined it is evident that the errors in the values
given by ODFAC are, on the average, as small as, if not
smaller than, those due to the rounding-off errors in-
herent in the strip methods.

Finally, by making all operations other than
recording the numerical values automatic, ODFAC eliminates
the ever-present source of error - the human error.

Conclusions. The chief advantages of ODFAC
are its ability to handle up to 31 coefficients in a
Fourier series and to perform the summation rapidly with
an accuracy adequate for most purposes. The simplicity
of the design of the machine virtually eliminates almost
all possibilities of electrical or mechanical failure. In
the event such failure should occur, all components are

Table 1

One-Dimensional Fourier Synthesis

Computed value	ODFAC	Deviation	Patterson-Tunell	Deviation	Beevers-Lipson	Deviation
30.0	31.4	+1.4	30	0	30	0
33.3	33.3	0	34	+0.7	35	+1.7
32.4	31.8	-0.6	32	-0.4	30	-2.4
17.2	15.5	-1.7	16	-1.2	16	-1.2
-0.3	0	-0.3	0	-0.3	0	-0.3
-4.0	-3.6	-0.4	-4	0	-2	-2.0
0.9	0	-0.9	-1	-1.9	-1	-1.9
2.5	1.5	-1.0	3	+0.5	4	+1.5
6.5	5.6	-0.9	7	+0.5	7	+0.5
24.1	23.6	-0.5	24	-0.1	24	-0.1
49.0	47.8	-1.2	50	+1.0	48	-1.0
70.5	70.0	-0.5	71	+0.5	72	+1.5
89.4	88.3	-1.1	89	-0.4	89	-0.4
110.9	111.0	+0.1	112	+1.1	113	+2.1
119.2	118.0	-1.2	120	+0.8	118	-1.2
98.0	98.5	+0.5	98	0	98	0
59.0	59.0	0	60	+1.0	60	+1.0
29.5	29.2	-0.3	28	-1.5	29	-0.5
17.6	16.0	-1.6	17	-0.6	17	-0.6
10.1	9.3	-0.8	9	-1.1	10	-0.1
3.0	1.0	-2.0	2	-1.0	4	+1.0
-0.7	-1.5	+0.8	-2	+1.3	-2	+1.3
-2.3	-3.1	+0.8	-3	+0.7	-5	+2.7

-9.9	-11.8	+1.9	-11	+1.1	-10	+0.1
-16.9	-17.9	+1.0	-17	+0.1	-17	+0.1
-4.0	-2.6	-1.4	-4	0	-2	-2.0
31.7	32.5	+0.8	32	+0.3	30	-1.7
66.6	66.7	+0.1	66	-0.6	66	-0.6
76.8	77.5	+0.7	76	-0.8	76	-0.8
66.1	68.5	+2.4	66	-0.1	67	+0.9
58.0	56.5	-1.5	58	0	58	0

readily accessible and removable for repair.

The slowest part of the operation of ODFAC lies in recording the results. It is proposed to add an automatic recorder for this purpose.

Extension to two dimensions

Use of two units. One ODFAC unit performs a
two-dimensional synthesis by means of a Beevers-Lipson
expansion. A combination of two such units performs
this summation more rapidly. If these units are equipped
with chart-type recorders, the most complicated two-
dimensional series having 30 x 30 Fourier coefficients
can be performed in an afternoon. The utilization of
two such units follows the plan indicated below.

The series to be summed has a general expression:

$$\rho(xy) = \sum_h \left[\sum_k F_{hk} \cos 2\pi(hx+ky) \right]$$

$$= \sum_h \left[\sum_k F_{hk} \cos 2\pi ky \right] \cos 2\pi hx - \sum_h \left[\sum_k F_{hk} \sin 2\pi ky \right] \sin 2\pi hx$$

The summations over k are first performed at the same
time by the two units working independently. The results
of these first summations are then used as coefficients
for the second summation over h. In the second operation
the two units are connected in parallel to only one recorder,
which thus records the results of the final two-dimensional
summation.

Two-dimensional computer. A more elaborate ex-
tension to two-dimensions can be built by combining two

To Recorde

R_4	R_0	R_4	R_1	R_4	R_2	R_4	R_3	R_4	R_4
R_3	R_0	R_3	R_1	R_3	R_2	R_3	R_3	R_3	R_4
R_2	R_0	R_2	R_1	R_2	R_2	R_2	R_3	R_2	R_4
R_1	R_0	R_1	R_1	R_1	R_2	R_1	R_3	R_1	R_4
R_0	R_0	R_0	R_1	R_0	R_2	R_0	R_3	R_0	R_4

0   1   2   3   4

$k \longrightarrow$
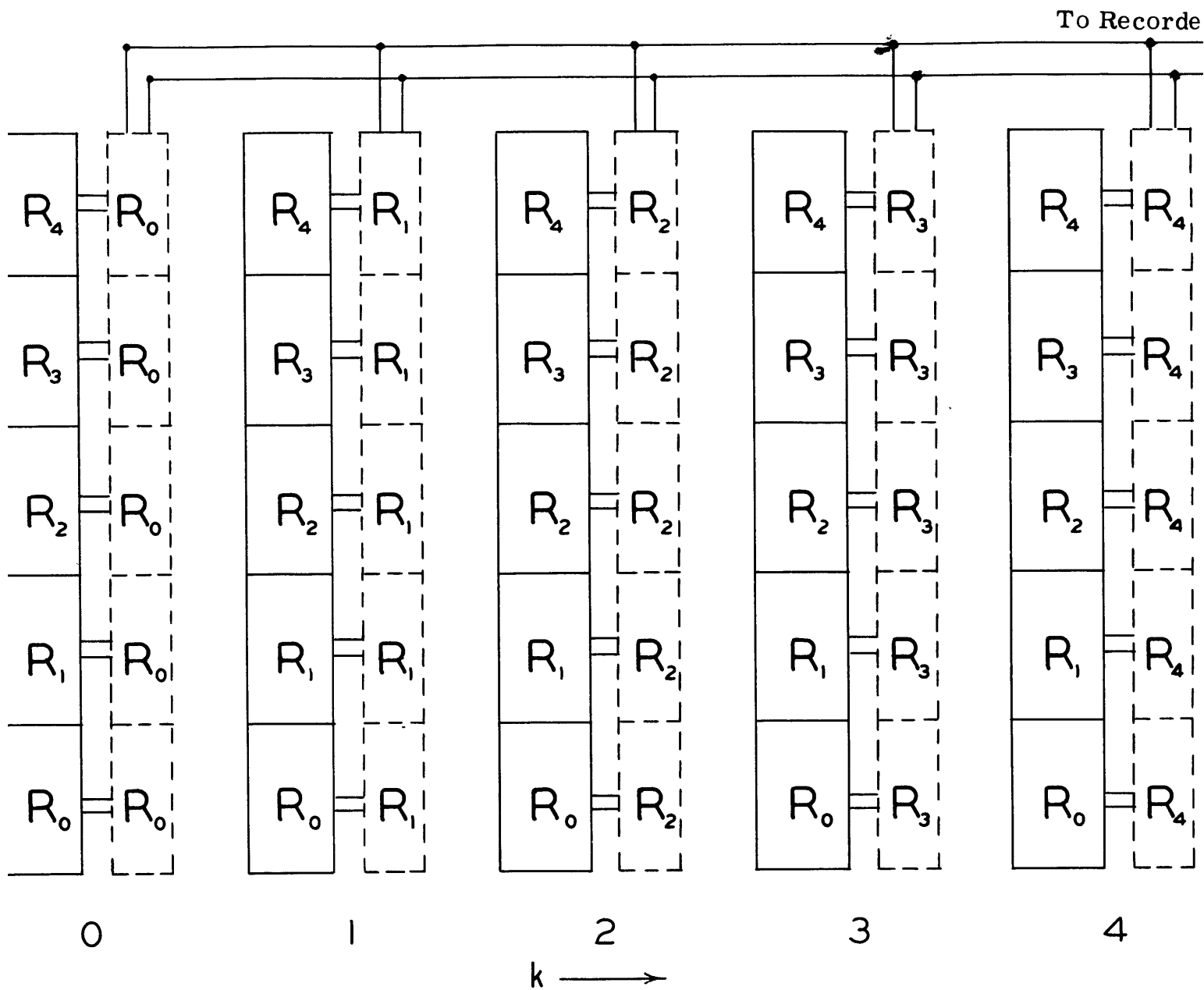
Fig. 10   Two-Dimensional Computer

resolvers for every term in the series. The construction entails building $\underline{k}$ ODFAC units and one "master" ODFAC having $\underline{h}$ resolvers (without variacs) for each harmonic $\underline{k}$. Such a plan is illustrated in Fig. 10 for $\underline{k} = \underline{h} = 4$.

The ODFAC units, whose resolvers have angular speed ratios proportional to their particular $\underline{h}$, are shown in solid lines. The rectangles in the dotted lines represent the resolvers of the "master" unit. All of these latter resolvers have the same angular settings proportional to $\underline{k}$.

The coupling between all units is electrical only. The resolvers of one ODFAC unit produce voltages proportional to:

$$F_{h_1 k_1} \cos 2\pi h_1 x$$

$$F_{h_2 k_1} \cos 2\pi h_2 x$$

$$F_{h_3 k_1} \cos 2\pi h_3 x$$

$$\cdot$$

$$\cdot$$

$$\cdot$$

which are fed to the resolvers, $\underline{R_k}$, of the master unit. The outputs of these resolvers are thus proportional to:

$$(F_{h_1 k_1} \cos 2\pi h_1 x) \cos 2\pi k_1 y$$

$$(F_{h_2 k_1} \cos 2\pi h_2 x) \cos 2\pi k_1 y \quad \text{etc.}$$

Appropriate electrical coupling of the resolvers in the master unit then produces a voltage proportional to

$$\sum_h \sum_k F_{hk} \cos 2\pi(hx + ky)$$

Part II. The Refinement of the Structure of Cubanite

Introduction

The crystal structure of cubanite was determined by M.J. Buerger[16] in 1947. The ferromagnetic property of cubanite and the possibility of its relationship to the structure of another ferromagnetic mineral, pyrrhotite, made the knowledge of the exact structure of cubanite of more than routine interest. For these reasons this writer decided to use the refinement of the structure of cubanite as a vehicle for demonstrating the application of the computer described in the first half of this thesis.

The space group of cubanite is $\underline{Pcmn}$. The cell constants reported by Buerger[16] are $\underline{a} = 6.46_3$ Å, $\underline{b} = 11.117$ Å, $\underline{c} = 6.233$ Å and were found to be in agreement with those determined from the measurements of the precession photographs taken in the course of this investigation. This cell contains 4 $CuFe_2S_3$.

In this part of the thesis the refinement procedure will be described, with special emphasis on the role ODFAC played in simplifying the attendant computations. The refinement was carried out in three stages. During the first stage successive Fourier refinements were carried out in the $(0\underline{kl})$ and $(\underline{hk}0)$ zones. In the second stage

the complete three-dimensional intensities were used to refine the x and z atomic coordinates with the aid of plane sections. In the third stage, three line sections were passed through each atom, and difference maps were used to determine the final atomic positions.

Experimental Procedure

Photographic Technique. The crystal selected
for intensity measurements came from the Frood Mine,
Sudbury, Ontario and is the same crystal that was used
by M.J. Buerger in the original structure determination[16].
The crystal was mounted on its $\underline{b}$ crystallographic axis
and placed on the Buerger precession [17] camera. The
($\underline{hk}0$) and ($0\underline{kl}$) zones were then photographed with moly-
bdenum $\underline{K}\alpha$ radiation and the intensities were measured
by the M.I.T. modification of the Dawton[18] method.

The complete set of three-dimensional intensities
was determined similarly. The individual levels of the
reciprocal lattice perpendicular to the $\underline{a}^*$ and $\underline{c}^*$ axes were
first photographed. Due to the blind area arising in the
center of upper-level precession photographs, it was
necessary to take additional photographs at another set-
ting. It turns out that for crystals having orthorhombic
symmetry all the missing intensities can be found on re-
ciprocal lattice planes perpendicular to $\underline{d}^*_{101}$ (see Fig.
11). It was therefore necessary to make only one additional
setting of the crystal to obtain all the intensities con-
tained in the limiting sphere of reflection.

The symmetry of the reciprocal lattice combined
with the repeated appearance of the same spots on more than

h,k, h+0
h,k, h+1
h,k, h+2
h,k, h+3

d^*_{101}

Shaded area represents
area swept out by $\underline{a}^*$
and $\underline{c}^*$ precession
photographs.
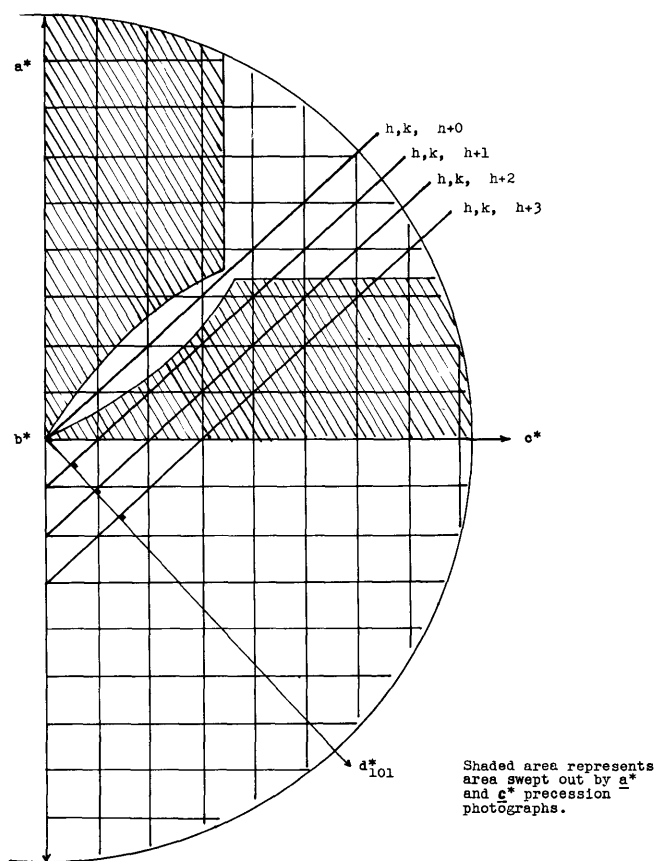
Fig. 11 Reciprocal Lattice

one photograph provided the possibility to make four in-
dependent measurements of approximately 70% of the observ-
able intensities. The remaining intensities were measured
independently at least twice. The averages of these
measurements were then used as the final observed inten-
sities.

Conversion of Intensities to Structure Factors.

The intensities were corrected by applying the Lorentz and polarization factors as determined for the zero-level precession photographs by Waser[19] and upper levels by Burbank[20] and Wells and Abrahams[21]. The charts prepared by the above-mentioned authors were enlarged to a radius of 10 cm. and printed on transparent film. These films were then placed over a reciprocal-lattice net drawn to the same scale. The use of these enlarged charts and reciprocal-lattice nets rather than the original films allows a more accurate and rapid determination of the value of the correction.

The intensities were next corrected for absorption by the crystal. Since the crystal was an irregular, jagged fragment, an exact determination of the absorption correction was nearly impossible. It was therefore decided to apply an absorption correction based on the assumption that the crystal was spherical. Although this assumption is not strictly valid, it was felt that such an absorption correction would, nevertheless, appreciably decrease the errors in the observed intensities due to absorption effects.

The absorption corrections made were based on a method suggested by Ekstein and Evans[22]. The radius r of the sphere is first determined. In this case the average radius of the crystal ($r = 0.0175$ cm.) was used.

The value of the radius is then multiplied by the linear
absorption coefficient of the crystal, in this case
μ_1 = 127.5 cm $^{-1}$. The per cent transmission as a function
of $\bar{\theta}$ can then be determined by forming the product
$\mu_1 \cdot r$ = 2.23) and referring to the above-cited tables.
The tables list the per cent of x-radiation transmitted
at the angles $\theta = 0^\circ$, $22\frac{1}{2}^\circ$, 45°, $67\frac{1}{2}$ and 90°. These
values are then plotted and the best curve drawn through
them. In this case the plot of transmissivity was made
against sin θ rather than θ as suggested by Evans[22], and
is shown in Fig. 12. The absorption correction was then
applied to the observed intensities by reading the per cent
transmitted corresponding to the value of sin θ for the
reflection concerned and dividing the observed intensity
by this value.

Finally, the square root of the corrected inten-
sities was taken and these values were used as the observed
structure factors. The observed structure factors were
placed on an absolute basis, by determining a temperature
factor and applying it to the computed structure factors.
The procedure used is described in Appendix I and the ob-
served structure factors are listed in Appendix II.

Transmission of X-Rays
Cubanite

15.0

Transmission (per cent)

10.0

5.0

0

0   .100   .200   .300   .400   .500   .600   .700

sinθ
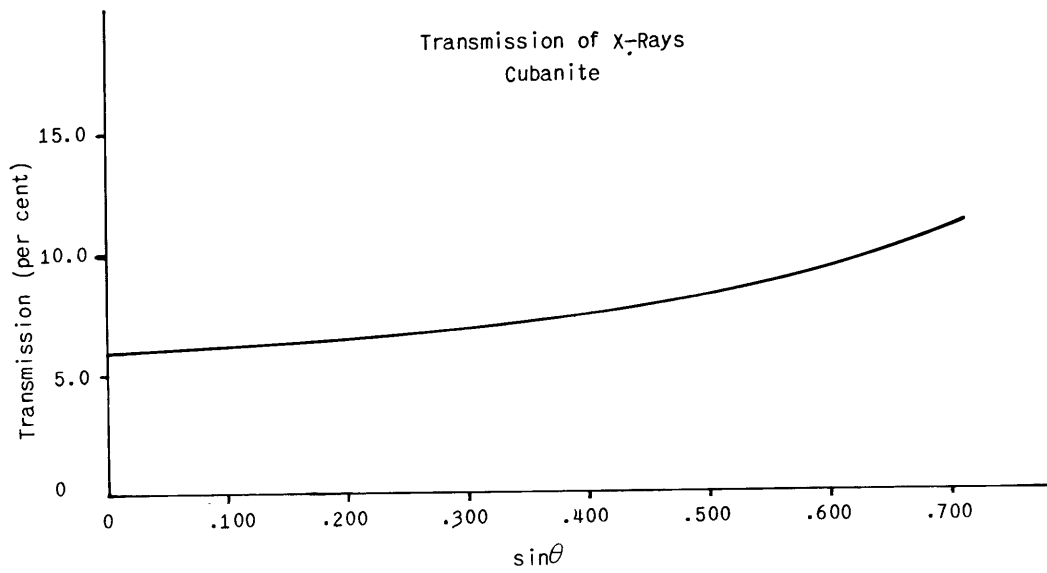
Fig.12 Absorbtion Correction Curve

Refinement of Coordinates

Refinement in Projection. The atomic coordinates determined by Buerger[16] (see Table II, pp. 56) were used as the starting point. The phases determined by these coordinates were used to compute the electron density $\rho(yz)$, Fig. 13.

The equation for this projection is:

for $l = 2n$

$$\rho(yz) = \frac{8}{A}\left\{ \sum_{\substack{k \\ 0}}^{\infty} \sum_{l} F_{0kl} \cos 2\pi ky \cos 2\pi lz \right.$$
$$k=2n$$

$$- \sum_{\substack{k \\ 0}}^{\infty} \sum_{l} F_{0kl} \sin 2\pi ky \sin 2\pi lz \quad *$$
$$k=2n+1$$

for $l = 2n+1$

$$\rho(yz) = 0$$

*In this equation and all those that follow x, y, z are fractional coordinates representing dimensionless ratios between the true distance from the origin in Angstroms and the parallel translation distances also expressed in Angstroms.

c/2

b/2
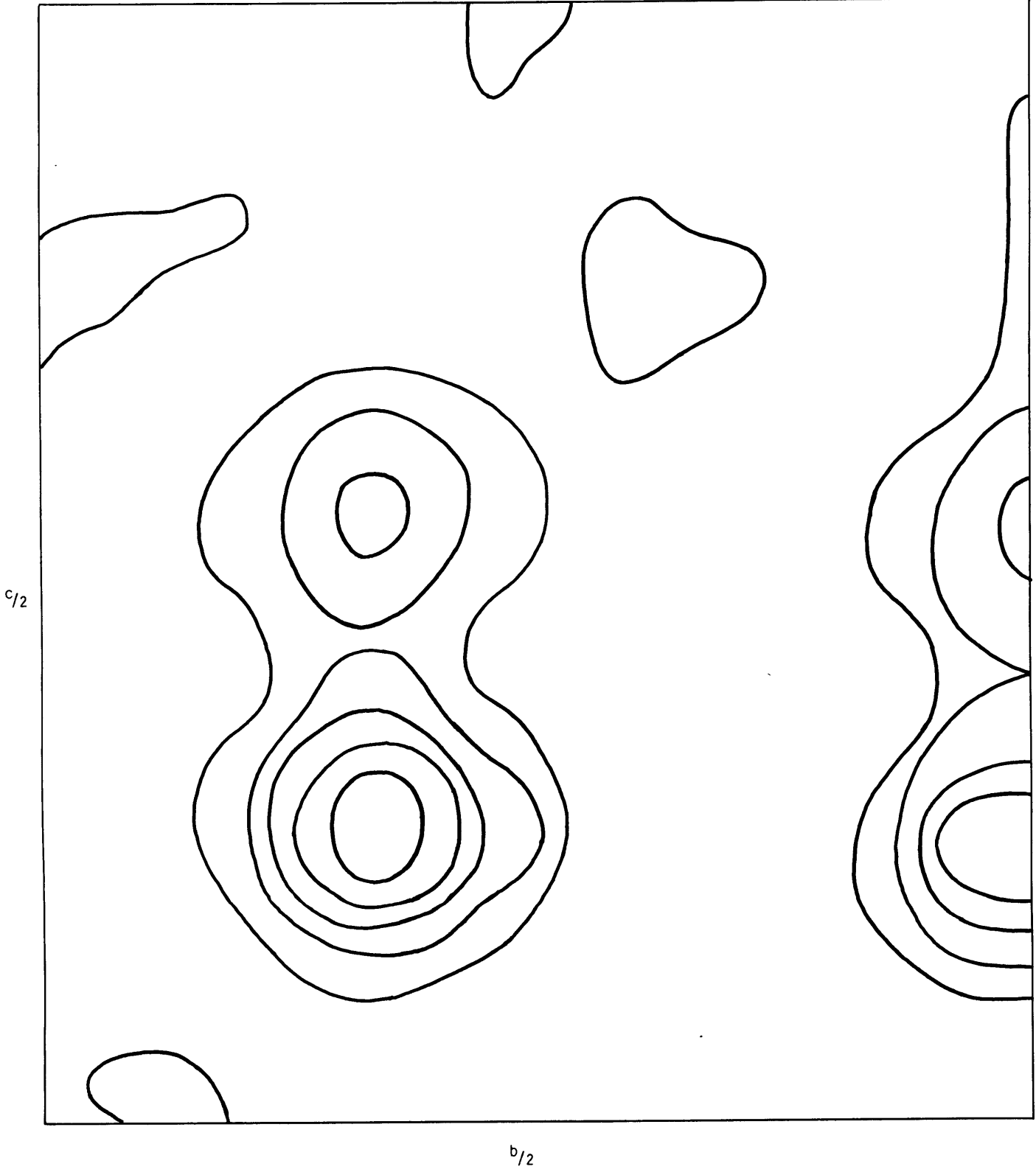
Fig.13 $\rho(yz)$

The appearance of only even values of $\underline{l}$ permits the actual synthesis to be carried out with a dummy index $\underline{l}' = \frac{l}{2}$. This has the effect of halving the true $\underline{c}$ axis and makes the sampling interval ($\underline{z} = \frac{1}{60}$) equal to $\frac{1}{120}$ of the true $\underline{c}$ axis.

As expected, the atoms are well resolved in this projection. The new atomic parameters (see Table II) were then used to compute a new set of structure factors. This new set gave a residual coefficient of 19% and showed no changes in phase for any reflection. It was therefore concluded that no further refinement was possible with this projection.

The new coordinates were then used to compute the structure factors for the ($\underline{hk}0$) reflections. These computations yielded a residual coefficient of 9.7% which was so low that it was felt that nothing could be gained by attempting a refinement in this projection, particularly since the $\underline{c}$ axis projection contains an overlap of each atom by another.

Refinement by Plane Sections. The possibilities
for refinement in projection thus being limited, it was
decided to continue the refinement in sections taken through
the crystal. Since the symmetry requires that two of the
four atoms in the asymmetric unit, viz., copper and sul-
phur$_1$, lie on the mirror plane perpendicular to the _b_
axis at $\underline{y} = \frac{1}{4}$, this plane was chosen as one of the sections
to be computed. The other two atoms, in the asymmetric unit,
iron and sulphur$_2$, lie on a plane perpendicular to _b_ at $\underline{y} =$
$\frac{1}{12}$ (see Fig. 13) and so this plane was chosen for the other
section.

The equation for ρ ($\underline{xyz}$) for the space group
$\underline{Pnma}$ is:[23]

$$\rho(xyz) = \frac{8}{V_c}\left\{ \sum_h^{h+l=2n} \sum_{k}^{\infty,\ k=2n} \sum_{l}_{0} F_{hkl} \cos 2\pi hx \cos 2\pi ky \cos 2\pi lz - \right.$$

$$\sum_h^{h+l=2n} \sum_{k}^{\infty,\ k=2n+1} \sum_{l}_{0} F_{hkl} \cos 2\pi hx \sin 2\pi ky \sin 2\pi lz -$$

$$\sum_h^{h+l=2n+1} \sum_{k}^{\infty\ k=2n} \sum_{l}_{0} F_{hkl} \sin 2\pi hx \cos 2\pi ky \sin 2\pi lz -$$

$$\left. \sum_h^{h+l=2n+1} \sum_{k}^{\infty\ k=2n+1} \sum_{l}_{0} F_{hkl} \sin 2\pi hx \sin 2\pi ky \cos 2\pi lz \right\}$$

When $\underline{y} = \frac{1}{4}$ this can be written in the form:

$$\rho \left(x\frac{1}{4}z\right) = \frac{8}{V_c}\left\{ \sum_l^{h+l=2n,\infty}\left[\sum_h^{k=2n} \left(\sum_k^{k=2n} F_{hkl}(-1)^{\frac{k}{2}} \right) \cos 2\pi hx - \right.\right.$$

$$\left. \sum_h^{h+l=2n=1,\infty} \left(\sum_k^{k=2n+1} F_{hkl}(-1)^{\frac{k-1}{2}} \right) \sin 2\pi hx \right] \cos 2\pi lz -$$

$$\sum_l^{h+l=2n,\infty}\left[\sum_h^{k=2n+1} \left(\sum_k F_{hkl}(-1)^{\frac{k-1}{2}} \right) \cos 2\pi hx + \right.$$

$$\left.\left. \sum_h^{h+l=2n+1,\infty} \left(\sum_k^{k=2n} F_{hkl}(-1)^{\frac{k}{2}} \right) \sin 2\pi hx \right] \sin 2\pi lz \right\}$$

When $\underline{y} = \frac{1}{12}$ the form of the equation is the same except that the summation over $\underline{k}$ takes the form:

when $\underline{k} = 2n$,

$$\sum_k F_{hkl} \cos \frac{2\pi k}{12}$$

when $\underline{k} = 2n+1$,

$$\sum_k F_{hkl} \sin \frac{2\pi k}{12}$$

As can be seen from the above equations the first summation to be performed is that over $\underline{k}$. This can be done most expediently with the help of some computational aid like the Patterson-Tunell strips[14]. Since only one value of $\underline{y}$ is required the time consumed setting the dials of ϴDFAC is greater in comparison.

The next step of the summation, on the other hand, can be carried out most efficiently by ODFAC. Since for any given value of $\underline{l}$, the terms having $\underline{h}$ odd or even are combined separately and then added, it is possible to put all the terms into the machine and by putting the selector switch on $\underline{\cos}_e + \underline{\sin}_o$ or $\underline{\cos}_o + \underline{\sin}_e$, as the case may be, perform both summations simultaneously and obtain their combined sum directly. The final summations over $\underline{l}$ are then performed in the usual manner.

The two sections $(\underline{x\tfrac{1}{4}z})$ and $(\underline{x\tfrac{1}{12}z})$ are shown in Figs. 14 and 15. As can be seen, the atoms are clearly resolved and are spherical in shape, indicating that the phases are correct. The weak background may be due to stray electrons or just to a cumulation of series termination errors.

The changes in the atomic parameters obtained from these two sections were very slight (see Table II). Only the weak intensities were recomputed at this stage,
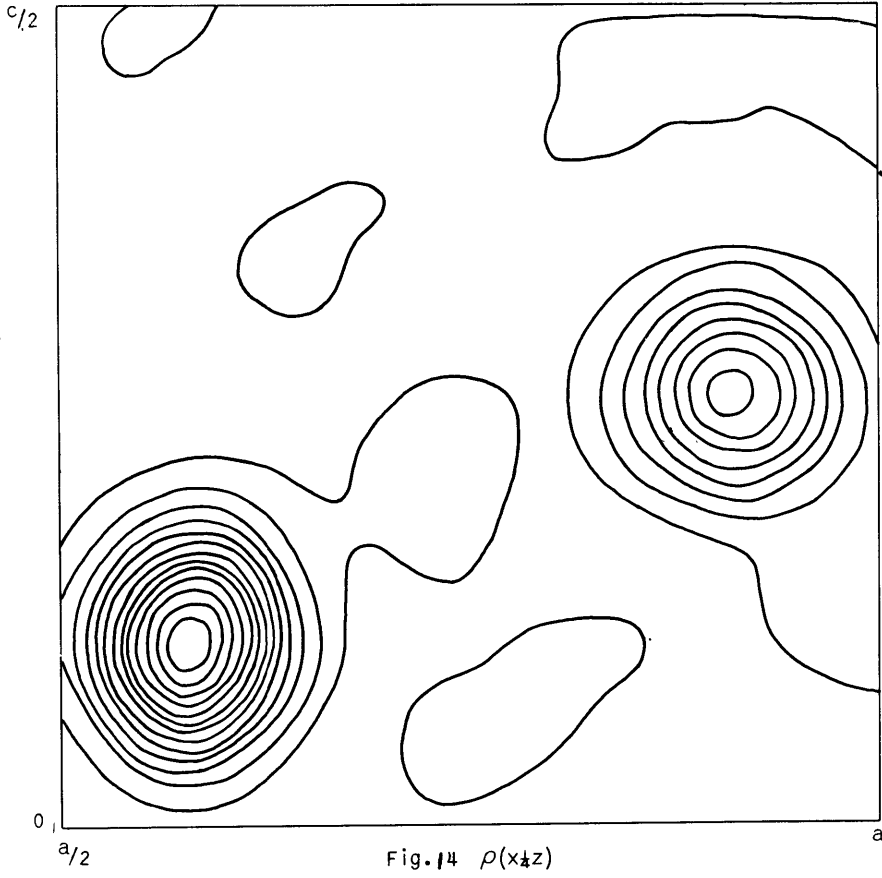
Fig.14 $\rho(x\frac{1}{4}z)$
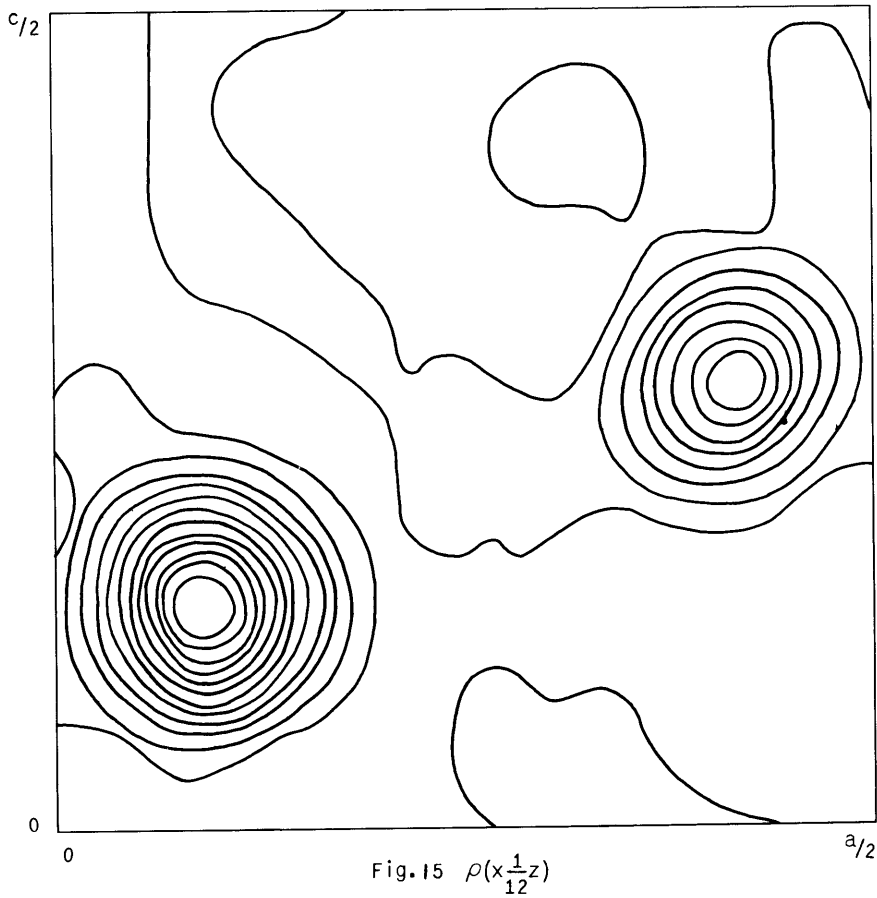
Fig.15 $\rho(x\frac{1}{12}z)$

and, since no phases changed, it was decided to proceed
with the refinement by means of line sections through the
individual atoms. The residual coefficient for the entire
three-dimensional set of intensities at this state was 14%.

Refinement by Line-Sections. The availability
of a one-dimensional computer strongly suggested that much
of the time spent in computing plane sections could be
saved by making instead line sections through the atoms.
At first thought it may appear that the location of the
centers of the atoms must be known rather well before a
line section can be expected to accurately locate the
center of the atom along that line. It turns out, how-
ever, that, due to the spherical symmetry of the electron
distribution about the atom, a line passed through a point
several tenths of an Angstrom away from the true center
still locates the densest accumulation of electrons (the
center) quite accurately.

A line section parallel to the a, b, c axes
was passed through each atom. Since two of the parameters
are held fixed, the values of x and z as determined by
the plane sections were used to first determine the values
of y for the two atoms (iron and sulphur$_2$) located in
general positions. The newly determined values of y were
then used in the computations of the other two line
sections. The complete set of twelve line sections is
shown in Figs. 16, 17, 18, and 19.

The forms of the equations used in computing the
line sections can be illustrated by the ones used for iron,
the others being identical except for the values of the

$\rho_o(x)$ x = .087

$\rho_c(x)$ x = .085

$\rho_o(y)$ y = .087

$\rho_c(y)$ y = .087

$\rho_o(z)$ z = .134

$\rho_c(z)$ z = .134
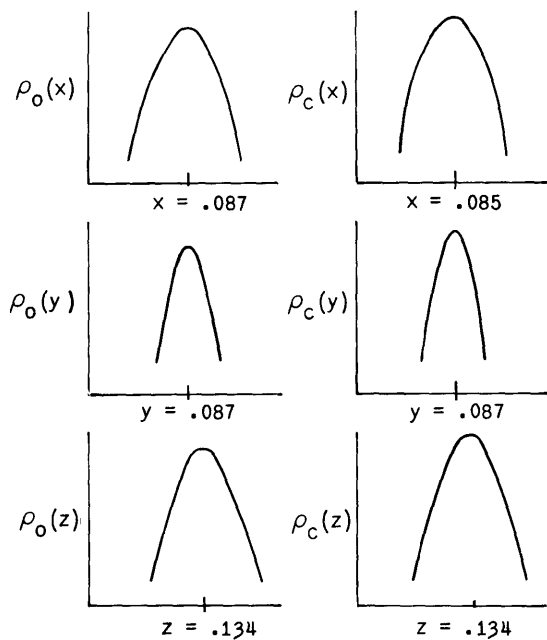
Fig. 16   Line Sections for Fe

$\rho_o(x)$ x = .413

$\rho_c(x)$ x = .415

$\rho_o(y)$ y = .084

$\rho_c(y)$ y = .083

$\rho_o(z)$ z = .274

$\rho_c(z)$ z = .274
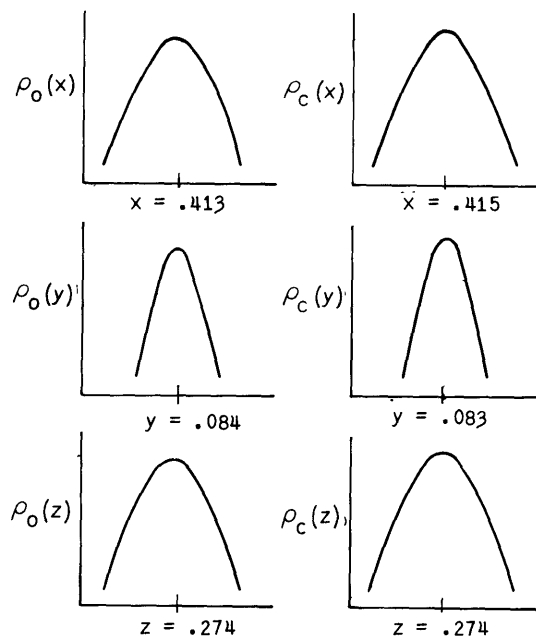
Fig. 17   Line Sections for S_{11}

$\rho_o(x)$ x = .583

$\rho_c(z)$ x = .583

$\rho_o(z)$ z = .127

$\rho_c(z)$ z = .127
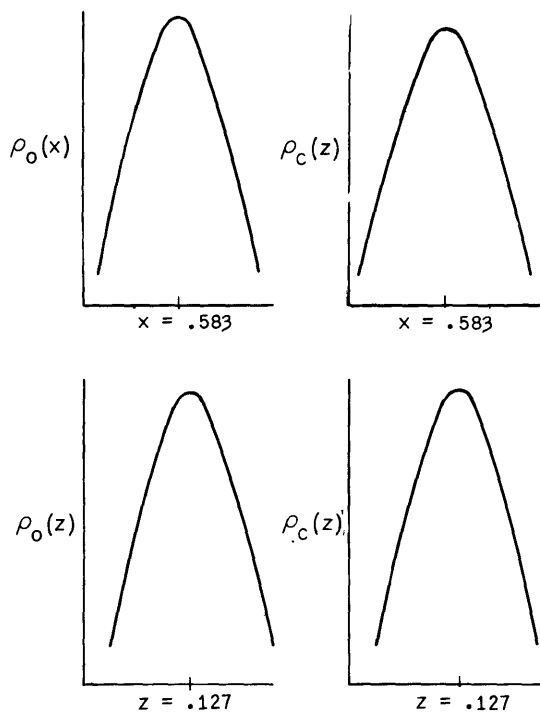
Fig. 18   Line Sections for Cu

$\rho_o(x)$ x = .913

$\rho_c(x)$ x = .913

$\rho_c(z)$ z = .262

$\rho_c(z)$ z = .268
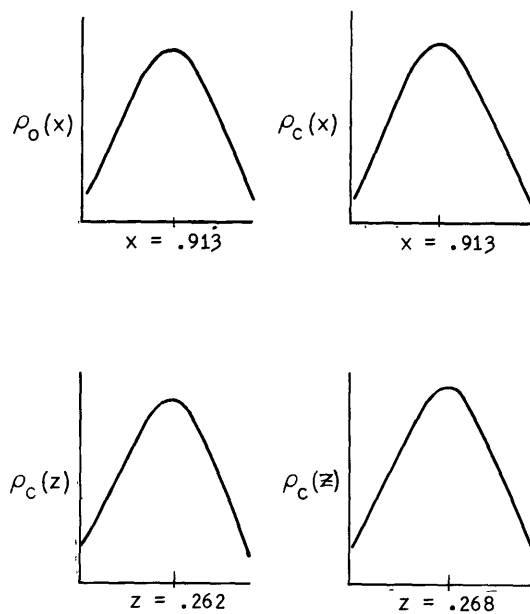
Fig. 19   Line Sections for S_1

respective $\underline{x}$, $\underline{y}$ and $\underline{z}$ coordinates.

For refining $\underline{y}$

$$\rho(\tfrac{5}{60}, y, \tfrac{8}{60}) = \frac{8}{V_c}\left\{ \overset{k=2n}{\underset{k}{\sum}} \left[\overset{h+l=2n}{\underset{h}{\sum}\underset{l}{\sum}} F_{hkl}\cos 2\pi h\tfrac{5}{60}\cos 2\pi l\tfrac{8}{60} - \right. \right.$$

$$\left. \overset{h+l=2n+1}{\underset{h}{\sum}\underset{l}{\sum}} F_{hkl}\sin 2\pi h\tfrac{5}{60}\sin 2\pi l\tfrac{8}{60}\right]\cos 2\pi ky -$$

$$\overset{k=2n+1}{\underset{k}{\sum}}\left[\overset{h+l=2n}{\underset{h}{\sum}\underset{l}{\sum}} F_{hkl}\cos 2\pi h\tfrac{5}{60}\sin 2\pi l\tfrac{8}{60} + \right.$$

$$\left. \left. \overset{h+l=2n+1}{\underset{h}{\sum}\underset{l}{\sum}} F_{hkl}\sin 2\pi h\tfrac{5}{60}\cos 2\pi l\tfrac{8}{60}\right]\sin 2\pi ky \right\}$$

The summations over $\underline{h}$ and $\underline{l}$ were carried out first with the aid of Patterson-Tunell strips. The summations over $\underline{k}$ were performed on ODFAC with the selector switch set on $\underline{cos}_e + \underline{sin}_o$. The sampling interval used was $\frac{1}{120}$ of a cell edge in all of these computations.

For refining $\underline{x}$

$$\rho(x,\tfrac{5}{60},\tfrac{8}{60}) = \tfrac{8}{V_o}\left[\overset{h+l=2n}{\underset{h}{\sum}}\left\{\overset{k=2n}{\underset{l}{\sum}}\left[(\underset{k}{\sum} F_{hkl}\,\cos\,2\pi k\tfrac{5}{60})\cos\,2\pi l\tfrac{8}{60}\right.\right.\right. -$$

$$\left.\left.\left.(\overset{k=2n+1}{\underset{k}{\sum}} F_{hkl}\,\sin\,2\pi k\tfrac{5}{60})\sin\,2\pi l\tfrac{8}{60}\right]\right\}\cos\,2\pi hx \right. -$$

$$\overset{h+l=2n+1}{\underset{h}{\sum}}\left\{\overset{k=2n}{\underset{l}{\sum}}\left[(\underset{k}{\sum} F_{hkl}\,\cos\,2\pi k\tfrac{5}{60})\sin\,2\pi l\tfrac{8}{60}\right.\right. +$$

$$\left.\left.(\overset{k=2n+1}{\underset{k}{\sum}} F_{hkl}\,\sin\,2\pi h\tfrac{5}{60})\cos\,2\pi l\tfrac{8}{60}\right]\right\}\sin\,2\pi hx \right]$$

The summations over $\underline{k}$ and $\underline{l}$ were carried out first with the aid of Patterson-Tunell strips. Since the summation over $\underline{k}$ will be required again for the section along $\underline{z}$, it was carried out first. The final summations over $\underline{h}$ were then performed on ODFAC.

For refining $\underline{z}$

$$\rho\left(\tfrac{-5}{60},\tfrac{-5}{60},z\right) = \frac{8}{V_c}\Bigg\{ \sum_l^{h+l=2n}\bigg[\sum_h^{k=2n}\Big(\sum_k F_{hkl}\cos 2\pi k\tfrac{5}{60}\Big)\cos 2\pi h\tfrac{5}{60}$$

$$-\sum_h^{\substack{h+l=2n+1\\k=2n+1}}\Big(\sum_k F_{hkl}\sin 2\pi k\tfrac{5}{60}\Big)\sin 2\pi h\tfrac{5}{60}\bigg]\cos 2\pi lz$$

$$-\sum_l^{h+l=2n}\bigg[\sum_h^{k=2n+1}\Big(\sum_k F_{hkl}\sin 2\pi k\tfrac{5}{60}\Big)\cos 2\pi h\tfrac{5}{60}$$

$$+\sum_h^{\substack{h+l=2n\\k=2n}}\Big(\sum_k F_{hkl}\cos 2\pi k\tfrac{5}{60}\Big)\sin 2\pi h\tfrac{5}{60}\bigg]\sin 2\pi lz\Bigg\}$$

The summation over $\underline{k}$ having been done before, only the summations over $\underline{h}$ and $\underline{l}$ remained. The summation over $\underline{h}$ can be done efficiently on ODFAC since for a given $\underline{l}$ the terms for $\underline{h}$ odd and even are combined separately and then added. The final summations over $\underline{l}$ were then also performed on ODFAC.

As can be seen from Figs. 16, 17, 18 and 19, the shifts in the atomic positions indicated by the line sections are very slight. It was therefore decided to use a more precise indication of the amount of movement required. To this end the "difference" electron densities suggested by Cochran[24] were used.

Since the line sections based on the observed structure factors had already been computed, it was decided to compute line sections using computed structure factors separately and then to subtract the two resulting electron densities to form the difference synthesis:

$$D = \rho_{obs.} - \rho_{calc.}$$

To this end scattering factors given by the Internationale Tabellen[25] were used. A temperature factor obtained by plotting $|F_o| / |F_o|$ as a function of $\sin^2\theta$ was applied to the computed structure factors so that they would be on the same scale as the observed structure factors. The procedure used is outlined in Appendix I.

The line sections based on the computed F's are also shown in Figs. 16, 17, 18, 19. As can be seen by comparing the electron densities based on observed and computed structure factors, the indicated shifts of the atomic centers were not always the same. The difference of the two electron densities was, therefore, plotted, and is shown in Fig. 20.

Cochran[24] gives criteria for computing the amount of shift required. Essentially, his equations state that the atom must be moved in the direction of the steepest gradient by an amount proportional to the steepness of the

$(\rho_o - \rho_c)_x$ $(\rho_o - \rho_c)_y$ $(\rho_o - \rho_c)_z$ $(\rho_o - \rho_c)_x$ $(\rho_o - \rho_c)_y$ $(\rho_o - \rho_c)_z$

Fe   x = .086   y = .088   z = .134   Fe   x = .087   y = .088   z = .134

Cu   x = .583   Special pos'n   z = .127   Cu   x = .583   Special pos'n   z = .127

S_I x = .913   Special pos'n   z = .262 S_I x = .913   Special pos'n   z = .262

S_{II} x = .415   y = .084   z = .274 S_{II} x = .413   y = .084   z = .274
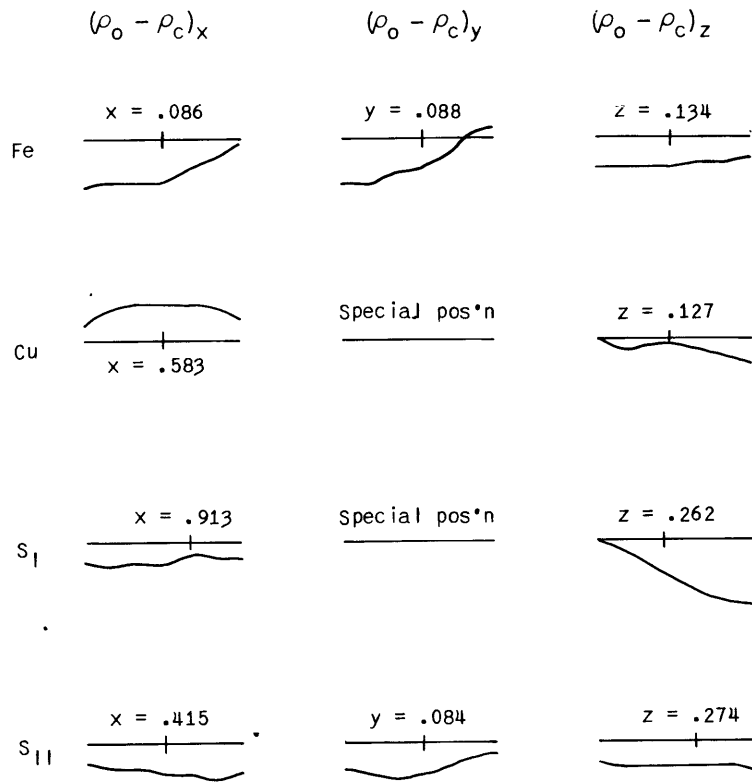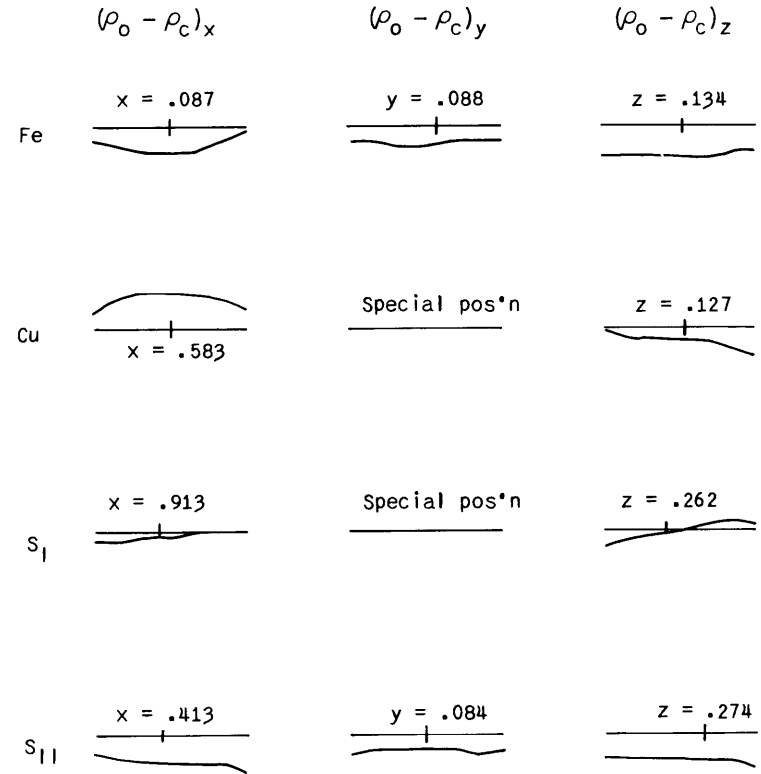
Fig. 20 Differential Syntheses   Fig. 21 Final Differential Syntheses

gradient. In this case an empirical relationship based on the measured gradient and the amount of shift indicated by the corresponding electron density plot was worked out and applied to all the atoms requiring a shift. Since the criterion for correctness of an atomic position is that the atom must be located on a slope of zero gradient, only those atoms situated on definitely sloping gradients were moved.

The resulting atomic coordinates (see Table II) were then used to compute structure factors for the two zones (hk0) and (0kl). The residual coefficients of 7.7% and 11.0% respectively, indicated that the refinement had been carried as far as experimentally available data would permit.

As a final check, the entire three-dimensional set of structure factors was computed and is tabulated along with the observed structure factors in Appendix II. The residual coefficient index for the entire set of structure factors is 11.9%. Difference syntheses based on these intensities were also computed, similarly to the ones above, and they are shown in Fig. 21. As can be seen from these plots these atomic positions can be assumed to be final.

Final Atomic Parameters. The final atomic
parameters and the corresponding residual coefficients
for the structure factors computed using these parameters
are tabulated in Table II. The table is constructed to
indicate the basis of selecting the parameters, the para-
meters thus determined, and the resulting residual co-
efficient for each set of parameters.

Table II

Parameter Changes

Basis for Parameters		Buerger's Original Structure	ρ (yz)	$\rho\,(x\tfrac{1}{4}z)$ $\rho\,(x\tfrac{1}{12}z)$	Line Syntheses	Difference Syntheses	Final Parameters
	x	$.083_5$	.083		.086	$.087_5$	$.087_5$
Fe	y	.083	.085	.088	.088	.088	.088
	z	.135	.136	.133	.134	.134	.134
	x	.583	.583		.583	.583	.583
Cu	y	1/4	1/4	1/4	1/4	1/4	1/4
	z	.122	.124	.130	.127	.127	.127
	x	.916	.916		.913	.913	.913
S_1	y	1/4	1/4	1/4	1/4	1/4	1/4
	z	.270	.264	.262	.262	.262	.262
	x	.417	.417		.415	.413	.413
S_2	y	.083	.084	.084	.084	$.083_5$	$.083_5$
	z	.265	.274	.274	.274	.274	.274
Residual Coefficient		(0kl) 22%	(hk0) 9.7%	(0kl) 19.0%	(0kl) 18%	(hkl) 14%	(hk0) 7.7% (0kl) 11.0%	(hkl) 11.9%

Discussion of Structure

The structure of cubanite is discussed in detail by Buerger[16]. "The structure [is] composed of slabs of the wurtzite arrangement parallel to (010) and averaging b/2 wide. Since the wurtzite arrangement is polar, the metal coordination tetrahedra all point up, or else they all point down. In the cubanite structure, the wurtzite-like slabs are joined to one another by inversion centers so that neighboring slabs have their tetrahedral apex directions reversed...Since the inversion center occurs at the midpoint of an edge of the iron tetrahedron, it has the effect of joining all iron tetrahedra in pairs which share this edge."

Since the sharing of a tetrahedral edge is most unorthodox and since this sharing occurs for iron tetrahedra only, it is difficult to avoid the correlation of this curious feature with the unusual characteristic of ferromagnetism. The reason for undertaking this re-finement procedure was, primarily, to learn more about the bond distributions in these iron tetrahedra.

The bond lengths and bond angles of the more important atoms are tabulated in Tables III and IV. The designations of the atoms refer to the illustration of the structure shown in Fig. 22. The shared edge of the iron tetrahedra is comprised of atoms labeled $S_2(D)$ and $S_2(E)$.
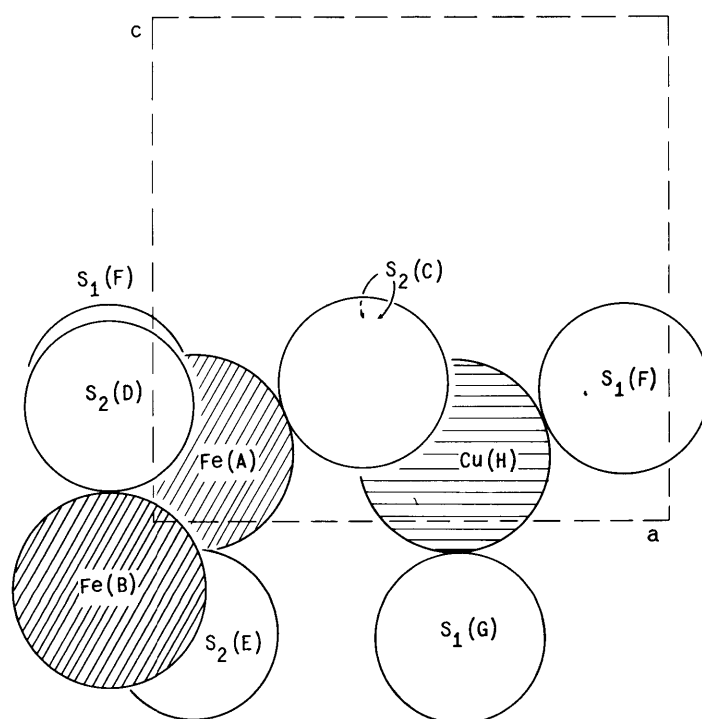
Fig. 22 Structural Unit

Table III

59.

Atom	Coordinates	Neighbor	Representative Coordinates	Bond Length
$\overline{Fe(A)}$	$x_1,\ y_1,\ z_1{}^*$	Fe(B)	$\bar{x}_1,\ \bar{y}_1,\ \bar{z}_1{}^*$	2.80_8 Å
		$S_2(C)$	$x_3,\ y_3,\ z_3$	2.27_8 Å
		$S_2(D)$	$1/2+x_3,\ \bar{y}_3, 1/2-z_3$	2.28_7 Å
		$S_2(E)$	$1/2-x_3,\ y_3, 1/2+z_3$	2.24_5 Å
		$S_1(F)$	$x_4, 1/4,\ z_4$	2.27_1 Å
Cu(H)	$x_2,\ y_2,\ z_2$	$2S_2(C)$	$x_3,\ y_3,\ z_3$	2.33_9 Å
		$S_1(F)$	$x_4, 1/4,\ z_4$	2.29_2 Å
		$S_1(G)$	$1/2-x_4, 1/4, 1/2+z_4$	2.27_5 Å
$S_2(D)$	$x_3,\ y_3,\ z_3$	Fe(A)	$x_1,\ y_1,\ z_1$	2.28_7 Å
		Fe(B)	$\bar{x}_1,\ \bar{y}_1,\ \bar{z}_1$	2.24_5 Å
		Fe	$1/2+x_1,\ \bar{y}_1, 1/2-z_1$	2.27_8 Å
		Cu(H)	$x_2, 1/4,\ z_2$	2.33_9 Å
		$S_2(D)$	$1/2+x_3,\ \bar{y}_3, 1/2-z_3$	3.84_4 Å
		$S_1(F)$	$x_4, 1/4,\ z_4$	3.85_7 Å
		$S_1(G)$	$1/2-x_4, 1/4, 1/2+z_4$	3.72_4 Å
$S_1(F)$	$x_4, 1/4,\ z_4$	Cu(H)	$x_2, 1/4,\ z_2$	2.29_2 Å
		Cu	$1/2-x_2, 1/4, 1/2+z_2$	2.27_5 Å
		$2Fe(A)$	$x_1,\ y_1,\ z_1$	2.27_1 Å
		$S_2(E)$	$1/2-x_3,\ y_3, 1/2+z_3$	3.73_4 Å
		$S_1(G)$	$1/2-x_4, 1/4, 1/2+z_4$	3.76_2 Å

* The subscripts 1,2,3,4 refer to the coordinates of Fe, Cu, S_{11}, S_1 respectively, as tabulated in Table II.

Table IV

Bonded Atoms	Angle
$S_2(D)-Fe-S_2(E)$	105° 36'
$S_2(C)-Fe-S_1(F)$	109° 57'
$S_2(C)-Fe-S_2(D)$	114° 44'
$S_1(F)-Fe-S_2(E)$	111° 35'
$S_2(C)-Cu-S_2(C)$	104° 38'
$S_2(C)-Cu-S_1(F)$	107° 03'
$S_1(F)-Cu-S_1(G)$	110° 54'
$S_2(C)-Cu-S_1(G)$	113° 12'

The length of this edge, $S_2(D)-S_2(E)=3.61$ Å is shorter

than the other S-S distances (3.84_4, 3.73_4, 3.85_7,

3.76_2 Å). The angle $S_2(D)-Fe-S_2(E)= 105^o$ 36' is less

than the tetrahedral angle of 109° 28' and is also less

than the other S-Fe-S angles (109° 57', 114° 44', $111^o35'$).

A somewhat similar distortion occurs for the copper tet-

rahedron. The copper atoms are located in symmetry planes

and are coordinated by two sulfur atoms in the same sym-

metry plane and two other sulfurs symetrically displaced

from the plane. The two sulfurs in the plane are each

shared by two copper and two iron atoms, whereas the sul-

fur atoms not lying in the symmetry plane are shared by

one copper and three iron atoms. The bond length from the

copper to these latter sulfurs is longer ($Cu-S_2(C)=2.33_9$Å)

than the Cu-S distances (2.29_2, 2.27_5Å) in the symmetry

plane and the angle between the bonds to two such sulfurs

($104^o38'$) is considerably smaller than the other S-Cu-S

angles ($107^o03'$, $110^o54'$, 113° 12').

The above, geometrical description of the struc-

ture can be used to draw some inferences regarding the re-

lationship between the bond distribution in cubazite and

the property of ferromagnetism. The ground state of iron

requires that 18 of its 26 electrons comprise the argon

core, six be in the 3d state and two in the 4s state. The

magnetic properties of the transition group elements are

attributed to the magnetic properties of the 3d electrons.
According to Slater[26] "... the required condition for ferro-
magnetism is that there be an inner partly-filled shell of
electrons, whose radius is as small as possible compared
with the interatomic distance." If we consider the Fe-S
distances, we find that one distance $(Fe-S_2(E)=2.24_5)$ is
shorter than the other three. Since the ionization potent-
ials of the 3d and the 4s electrons (.60 and .58) are nearly
the same, it is reasonable to assume that the four tetra-
hedral bonds of iron are formed by three unpaired 3d elec-
trons and one unpaired 4s electron, one of the 4s electrons
of the ground state having been raised to the 3d state.
This bond distribution is opposed to an earlier explana-
tion of the ferromagnetism of cubanite[27] which postulated
an Fe-Fe bond leaving one unpaired electron. In addition
to the lower potential energy attained by pairing all the
electrons, the shortening of the shared edge of the iron
tetrahedra casts serious doubt on the validity of this
earlier view.

ACKNOWLEDGEMENT

Bibliography

[1] C. A. Beevers. A machine for the rapid summation of
    Fourier series.
    Proc. Phy. Soc. 51 (1939) 660-667

[2] Douglas Macewan and C. A. Beevers. A machine for the
    rapid summation of Fourier series.
    J. Sci. Inst. (10) 19 (1924) 150-156.

[3] G. Hägg and T. Laurent. A machine for the summation
    of Fourier series.
    J. Sci. Inst. (7) 23 (1946) 155-158.

[4] I.W. Ramsay, H. Lipson, and D. Rogers. An electrical
    analogue machine for Fourier synthesis.
    Computing Methods and the Phase Problem in
    X-Ray Crystal Analysis (X-Ray Crystal Analysis
    Laboratory, The Pennsylvania State College),
    1952, 130-131.

[5] Dan McLachlan, Jr. and E. F. Champaygne. A machine
    for the application of sand in making Fourier
    projections of crystal structures.
    J. Ap. Phys. (12) 17 (1946) 1006-1014.

[6] A. J. Rose. Machine a calculer permettant la determina-
    tion de fonctions peiodiques et luer introduc-
    tion dans des calculs. Application a la sommation
    des series de Fourier et au calcul des facteurs

de structure en cristallographie.

Journal de Recherches, No. 7.

7 V. Vand. A Fourier electron-density balance.

J. Sci. Inst. 29 (1952) 118-121.

8 C. A. Beevers and J. Monteath Robertson. A multi-
component integrator for Fourier analysis and
structure factor calculator.
Computing Methods and the Phase Problem in
X-Ray Crystal Analysis (X-Ray Crystal Analysis
Laboratory, The Pennsylvania State College),
(1952) 119-129.

9 J. Monteath Robertson. A simple harmonic continuous
calculating machine.
Phil. Mag. (7) 13 (1932) 413-419.

10 R. Pepinsky. An electronic computer for x-ray crystal
structure analyses.
J. Ap. Phys. (7) 18 (1947) 601-604.

11 Ray Pepinsky. X-Rac and S-Fac; electric analogue
computers for x-ray analysis.
Computing Methods and the Phase Problem in
X-Ray Crystal Analysis (X-Ray Crystal Analysis
Laboratory, The Pennsylvania State College),
(1952) 167-390.

12 H. Shimizu, P. J. Elsey, and D. McLachlan, Jr. A
machine for synthesizing two-dimensional Fourier
series in the determination of crystal structures.
Rev. Sci. Inst. (9) 21 (1950) 779-783.

13 M. J. Buerger. Fourier summations for symmetrical crystals.

Amer. Mineral. 34 (1949) 771-788.

14 A. L. Patterson and George Tunell. A method for the summation of the Fourier series used in the x-ray analysis of crystal structures.

Amer. Mineral. 27 (1942) 655-679.

15 H. Lipson and C. A. Beevers. An improved numerical method of two-dimensional Fourier synthesis for crystals.

Proc. Phys. Soc. 48 (1936) 772-780.

16 M. J. Buerger, The Crystal Structure of Cubanite.

Amer. Min. 32 (1947) 415-425.

17 M. J. Buerger. The photography of the Reciprocal Lattice.

ASXRED Monograph. No. 1.

18 R.H.V.M. Dawton. The Interpretation of Large Numbers of X-Ray Crystal Reflections.

Proc. Phys. Soc. 50 (1938) 919-925.

19 J. Waser. Lorentz and Polarization Correction for the Buerger Precession Method.

Rev. of Sci. Inst. 22 (1951) 567-568.

20 R. D. Burbank. Upper Level Precession Photography and the Lorentz-Polarization Correction. Part I.

Rev. of Sci. Inst. 23 (1952) 321-327

21 H. J. Grenville-Wells and S. C. Abrahams. Upper Level
        Precession Photography and the Lorentz-Polari-
        zation Correction, Part II.
        Rev. of Sci. Inst. 23 (1952) 328-331.

22 M. G. Ekstein and H. T. Evans, Tables of Absorption
        Factors for Spherical Crystals.
        Phillips Laboratories Technical Report, No. 40.

23 International Tables for X-Ray Crystallography. Edited
        by N.F.M. Henry and K. Lonsdale, 1952. Kynoch
        Press. Birmingham, England.

24 W. Cochran. The Structures of Pyrimidines and Purines:V.
        The Electron Distribution in Adenine Hydrochloride.
        Acta. Cryst. 4 (1950) 81-92.

25 Internationale Tabellen zur Bestimmung von Kristall-
        struckturen. 1935. Gebrueder Borntraeger, Berlin.

26 J. C. Slater. Quantum Theory of Matter. 1951. McGraw-
        Hill Book Co. New York, N.Y. pp. 426.

27 A. F. Wells. Structural Inorganic Chemistry. Second
        Edition. 1950. Oxford, England. pp. 403.

APPENDIX I

Temperature Factor Determination

To facilitate the comparison of observed and computed structure factors they must be placed on the same scale. If the structure is correct, the ratio between the observed structure factors, measured on an arbitrary scale, and the computed structure factors should be constant, i.e.

$$\frac{\left|F_o\right|}{\left|F_c\right|} = k$$

The assumption that the atoms are at rest, made in computing the structure factors, is not valid at room temperatures. If a temperature factor is introduced to correct for the thermal motion of the atoms, the ratio between observed and computed structure factors becomes:

$$\frac{\left|F_o\right|}{\left|F_c\right|} = k \ \exp\left(-2B \ \frac{\sin^2\theta}{\lambda^2}\right)$$

or

$$\log_e \frac{\left|F_o\right|}{\left|F_c\right|} = \log_e k - 2B \ \frac{\sin^2\theta}{\lambda^2}$$

The later equation is an equation of a straight line and is useful in determining the value of $\underline{B}$, the

unknown quantity in the above equation.

Since the temperature factor is a function of $\sin^2\theta$ it is convenient, in practice, to first compute the ratio between $\left|F_o\right|$ and $\left|F_c\right|$ and then to determine the average value of this ratio for limited ranges of $\sin^2\theta$. A plot of these values vs $\sin^2\theta$ is then used to determine the temperature correction.

The actual plot used in this case is represented by Fig. 23 which shows the plot of $\text{Log}_e \dfrac{\left|F_o\right|}{\left|F_c\right|}$ vs $\sin^2\theta$ for the final set of computed structure factors. The accompanying tables show the details of the computations.

The final computed structure factors, on an absolute basis, are listed along with the observed structure factors in Appendix II.
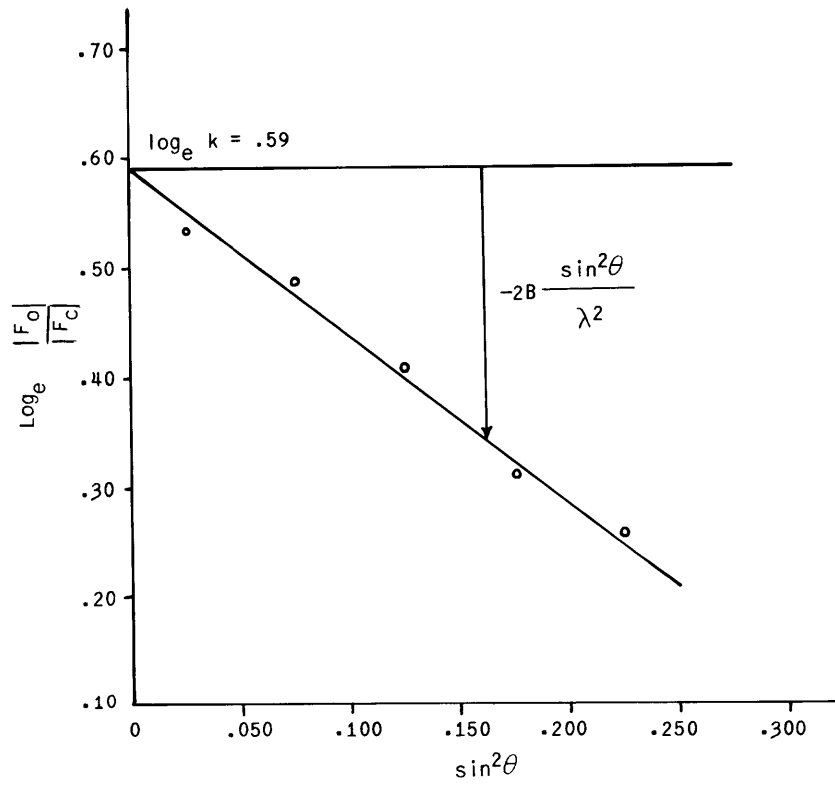
Fig. 23 Temperature Correction

$$0 \left\langle \sin^2\theta \right\rangle .050$$

hkl			$\sin^2\theta$	$|F_0|$	$|F_c|$	$k=\dfrac{|F_0|}{|F_c|}$
0	2	0	.004	4	5 1/2	.73
0	6	0	.020	34	79 1/2	.43
1	3	0	.012	25 1/2	51 1/2	.50
2	0	0	.012	23 1/2	47	.50
2	2	0	.016	1 1/2	3	.50
2	6	0	.048	17 1/2	34 1/2	.49
3	3	0	.037	32	79 1/2	.40
4	0	0	.048	18	41 1/2	.43
1	0	1	.006	7	13	.54
1	2	1	.010	14 1/2	27 1/2	.53
1	3	1	.016	7	11	.63
1	4	1	.23	14	27	.52
1	6	1	.043	4	8 1/2	.47
2	0	1	.016	12	11	1.10
2	1	1	.017	15 1/2	27 1/2	.56
2	3	1	.025	5	11 1/2	.44
2	5	1	.041	11	19 1/2	.56
0	0	2	.013	18	38 1/2	.47
0	1	2	.014	18	39	.46
0	3	2	.022	7	11 1/2	.61
0	5	2	.037	16 1/2	26 1/2	.62
0	6	2	.048	15	29 1/2	.51

hkl			$\sin^2\theta$	$\|F_o\|$	$\|F_o\|$	$F=\dfrac{\|F_o\|}{\|F_o\|}$
1	0	2	.016	5	7	.71
1	2	2	.020	10	17	.59
1	3	2	.026	10 1/2	17 1/2	.60
1	4	2	.032	10	18	.56
2	0	2	.026	10	15 1/2	.65
2	1	2	.026	12	17	.71
3	0	2	.040	6 1/2	9 1/2	.68
3	2	2	.045	15	27 1/2	.55
1	0	3	.032	8	17	.47
1	2	3	.036	12	27 1/2	.44
1	3	3	.042	21	48	.44
1	4	3	.049	13	28 1/2	.46
2	0	3	.041	24 1/2	50	.49
2	1	3	.043	14 1/2	28 1/2	.51

Average value of $\underline{k}$ ~   .53$_7$

$$.050 \langle \sin^2\theta \rangle .100$$

hkl			$\sin^2\theta$	$|F_o|$	$|F_c|$	$k=\dfrac{|F_o|}{|F_c|}$
1	9	0	.086	15 1/2	32 1/2	.48
3	5	0	.054	3	6 1/2	.46
4	6	0	.086	14	35 1/2	.40
5	3	0	.086	11	27	.41
1	8	1	.073	7 1/2	15 1/2	.48
2	6	1	.053	4 1/2	7 1/2	.60
2	7	1	.067	10	22 1/2	.44
4	0	1	.051	5	8 1/2	.59
4	1	1	.053	9	20 1/2	.44
4	3	1	.061	4	7	.57
4	5	1	.078	7	16	.44
4	6	1	.089	2	6 1/2	.31
5	0	1	.077	3	9	.33
5	2	1	.082	8 1/2	18	.47
5	3	1	.087	8	6	1.33
5	4	1	.095	8 1/2	19 1/2	.44
0	7	2	.063	15 1/2	31 1/2	.49
0	9	2	.096	4	6 1/2	.61
1	6	2	.053	2	4 1/2	.44
1	8	2	.082	5	10	.50
1	9	2	.099	7	12 1/2	.56
2	5	2	.051	6	12	.50
2	6	2	.063	6	12 1/2	.48

hkl			$\sin^2\theta$	$|F_o|$	$|F_c|$	$k\dfrac{|F_o|}{|F_c|}$
2	7	2	.075	7	14 1/2	.48
3	3	2	.051	14 1/2	29	.50
3	4	2	.057	15 1/2	30 1/2	.51
3	6	2	.063	5	7 1/2	.67
4	0	2	.063	7	16 1/2	.42
4	1	2	.063	6 1/2	14 1/2	.41
4	5	2	.089	5 1/2	11	.50
4	6	2	.099	6 1/2	14	.46
5	2	2	.093	6	10 1/2	.57
5	3	2	.097	5	10	.50
1	6	3	.070	7	13 1/2	.52
1	8	3	.097	7	18	.39
2	3	3	.051	8	16	.50
2	5	3	.067	10	22	.45
2	6	3	.078	20	42	.48
2	7	3	.091	12	26	.46
4	0	3	.078	18	39 1/2	.46
4	1	3	.079	8 1/2	23	.37
4	3	3	.088	6 1/2	12	.54
0	0	4	.052	13	24	.54
0	6	4	.088	7	20	.35
1	3	4	.063	5	11 1/2	.43
2	0	4	.063	6 1/2	11	.59

hkl	$\sin^2\theta$	$|F_o|$	$|F_c|$	$k=\dfrac{|F_o|}{|F_c|}$
2 3 4	.088	8	20 1/2	.39
1 2 5	.088	4	6 1/2	.62
1 3 5	.093	17 1/2	44	.44
1 4 5	.099	4 1/2	7 1/2	.60
2 0 5	.092	21	45	.47
2 1 5	.092	5	7	.71

The average of $\underline{k}$ $=$ $.41_5$

$$.100 \ \langle \sin^2\theta \rangle \ .150$$

hkl	$\sin^2\theta$	$|F_o|$	$|F_c|$	$k\dfrac{|F_o|}{|F_c|}$
0 12 0	.144	17 1/2	53	.33
3 9 0	.110	24 1/2	58 1/2	.42
6 0 0	.110	22 1/2	59	.41
6 6 0	.140	18 1/2	53 1/2	.42
1 10 1	.111	7 1/2	19 1/2	.39
2 11 1	.144	4	11 1/2	.35
4 7 1	.104	9	18 1/2	.49
5 6 1	.116	2 1/2	7 1/2	.33
5 8 1	.143	4	13	.31
0 11 2	.136	8	15	.53
1 10 2	.119	6	14	.43
3 8 2	.106	8 1/2	18	.47
3 9 2	.124	10	23	.43
3 10 2	.138	9	26	.35
4 7 2	.112	6	14	.43
5 4 2	.104	6 1/2	11 1/2	.57
6 0 2	.122	8	22 1/2	.36
6 1 2	.124	10	22 1/2	.44
6 3 2	.132	3	6 1/2	.46
1 9 3	.114	13	36	.36
1 10 3	.135	8	23 1/2	.34
2 9 3	.124	6	12	.50

hkl	$\sin^2\theta$	$|F_o|$	$|F_c|$	$k=\dfrac{|F_o|}{|F_c|}$
4 5 3	.104	7 1/2	18 1/2	.41
4 6 3	.116	14	34	.41
4 7 3	.130	7 1/2	22 1/2	.33
5 0 3	.104	6	14	.43
5 2 3	.110	6	21	.29
5 3 3	.114	14	38	.37
5 4 3	.124	9	23	.39
5 6 3	.144	4	12 1/2	.32
2 6 4	.100	4	9 1/2	.42
4 0 4	.101	3 1/2	10	.35
2 6 5	.130	16 1/2	40 1/2	.41
4 0 5	.134	15	38 1/2	.39
4 3 5	.138	14	4	--
0 0 6	.116	3 1/2	6	.58
0 1 6	.117	11	.34	.32
0 2 6	.120	3	5	.60
0 3 6	.123	5 1/2	16 1/2	.33
0 4 6	.130	3	5 1/2	.55
0 5 6	.140	7	28	.25
1 2 6	.122	5	16	.31
1 4 6	.135	5 1/2	17	.32
2 1 6	.130	5 1/2	15 1/2	.35
3 0 6	.144	7	16	.44

The average value of __k__   = $.40_2$

$$.150 \ \langle \sin^2\theta \ \rangle \ .200$$

hkl	$\sin^2\theta$	$|F_o|$	$|F_c|$	$k=\dfrac{|F_o|}{|F_c|}$
2 12 0	.159	9	24	.38
4 12 0	.199	6 1/2	26	.25
4 9 0	.160	6	22	.27
7 3 0	.158	11	31 1/2	.35
8 0 0	.193	6	18 1/2	.32
2 13 1	.192	6	17	.35
5 10 1	.182	4 1/2	17 1/2	.26
7 2 1	.154	5	13 1/2	.37
7 4 1	.168	5	14 1/2	.35
0 12 2	.160	9	21	.43
0 13 2	.193	8	24 1/2	.33
6 5 2	.150	5	17 1/2	.29
6 6 2	.161	8 1/2	20 1/2	.41
6 7 2	.175	7 1/2	22 1/2	.33
7 3 2	.170	3 1/2	12 1/2	.28
1 12 3	.178	1	9	.11
2 11 3	.166	4	14	.29
2 12 3	.188	11 1/2	31	.37
4 9 3	.161	3	9 1/2	.32
5 8 3	.171	4	13	.31
5 9 3	.186	10	32	.31
7 2 3	.182	4	16	.25

hkl	$\sin^2\theta$	$\lvert F_o \rvert$	$\lvert F_c \rvert$	$k = \dfrac{\lvert F_o \rvert}{\lvert F_c \rvert}$
7 3 3	.186	8 1/2	28 1/2	.32
7 4 3	.195	5	17 1/2	.29
0 12 3	.198	4	14 1/2	.28
3 9 4	.160	5	16	.31
1 9 5	.168	13	35 1/2	.37
5 3 5	.166	11	38 1/2	.29
0 6 6	.152	3	5 1/2	.55
0 7 6	.167	10	33	.30
0 9 6	.198	4 1/2	13	.35
1 8 6	.194	3	12	.25
2 5 6	.152	3 1/2	13	.27
2 7 6	.176	5	15	.33
3 4 6	.160	12	32	.38
3 6 6	.178	4 1/2	14	.32

The average value of $\underline{k}$ = .32$_9$

hkl	$.200 \langle \sin^2\theta \rangle .250$			$k = \dfrac{\lvert F_o \rvert}{\lvert F_c \rvert}$
	$\sin^2\theta$	$\lvert F_o \rvert$	$\lvert F_c \rvert$	
1 15 0	.231	4	22	.18
7 9 0	.230	7	26 1/2	.26
8 6 0	.230	5	17	.29
4 13 1	.236	3 1/2	15	.23
2 13 3	.205	6	21	.29
4 11 3	.204	3	12 1/2	.24
4 12 3	.224	8	27	.26
5 10 3	.207	6	21	.29
8 0 3	.223	9	30 1/2	.29
8 1 3	.224	4 1/2	17 1/2	.26
2 12 5	.240	11	31	.35
5 9 5	.338	11	32 1/2	.34
1 10 6	.222	4	15 1/2	.26
3 8 6	.210	6 1/2	22 1/2	.29
3 10 6	.250	8 1/2	29	.29
6 1 6	.225	6 1/2	26	.25
0 0 8	.208	12	36 1/2	.33
0 1 8	.208	3	14	.22
0 3 8	.212	5	14 1/2	.35
1 3 8	.212	6	18 1/2	.32
2 0 8	.220	6	17	.35

hkl	$\sin^2\theta$	$\lvert F_o \rvert$	$\lvert F_c \rvert$	$k = \dfrac{\lvert F_o \rvert}{\lvert F_o \rvert}$
3 0 8	.233	4 1/2	14	.32
3 3 8	.233	10 1/2	34 1/2	.30

The average value of k   = $.28_5$

Appendix II

Final Structure Factors

This table lists all the observed and computed structure factors placed on an absolute basis as described in Appendix I.

A comparison of the observed and computed structure factors shows an agreement as good as the experimental data warrants. The largest disagreement occurs for the two strongest reflections (060) and (330) and is probably due to extinction for which no correction has been made.

hkl			F_{obs}	F_{calc}		hkl			F_{obs}	F_{calc}
0	2	0	4	− 3		1	0	1	7	7
0	6	0	34	−43		1	2	1	14 1/2	15
0	12	0	17 1/2	19 1/2		1	3	1	7	− 6 1/2
1	3	0	25 1/2	−28		1	4	1	14	−14 1/2
1	9	0	15 1/2	15		1	6	1	4	− 4
1	15	0	4	−6		1	8	1	7 1/2	−7 1/2
2	0	0	23 1/2	26		1	10	1	7 1/2	8
2	2	0	1 1/2	− 1 1/2		2	0	1	12	− 6 1/2
2	6	0	17	−18		2	1	1	15 1/2	−15
2	12	0	9	8 1/2		2	3	1	5	− 5 1/2
3	3	0	32	−42		2	5	1	11	−10
3	5	0	3	3 1/2		2	6	1	4 1/2	4
3	9	0	24 1/2	24 1/2		2	7	1	10	11
4	0	0	18	−21 1/2		2	11	1	4	4 1/2
4	6	0	14	16		2	13	1	6	− 5 1/2
4	12	0	6 1/2	− 7 1/2		4	0	1	5	− 4 1/2
5	3	0	11	−12 1/2		4	1	1	9	−10 1/2
5	9	0	6	7 1/2		4	3	1	4	− 3 1/2
6	0	0	22 1/2	−25		4	5	1	7	− 7 1/2
6	6	0	18 1/2	20		4	6	1	2	3
7	3	0	11	11		4	7	1	9	8 1/2
7	9	0	7	− 7 1/2		4	13	1	3 1/2	− 4
8	0	0	6	− 5 1/2		5	0	1	3	− 4
8	6	0	5	5		5	2	1	8 1/2	− 8 1/2

hkl	F_{obs}	F_{calc}		hkl	F_{obs}	F_{calc}
5 3 1	8	3		1 9 2	7	− 5 1/2
5 4 1	8 1/2	8 1/2		1 10 2	6	− 6
5 6 1	2 1/2	3		2 0 2	10	− 9
5 8 1	4	5		2 1 2	12	− 9 1/2
5 10 1	4 1/2	− 5 1/2		2 5 2	6	− 6
7 2 1	5	− 5		2 6 2	6	6
7 4 1	5	5		2 7 2	7	7
0 0 2	18	− 21		3 0 2	6 1/2	− 3 1/2
0 1 2	18	− 21		3 2 2	15	− 14 1/2
0 3 2	7	− 6 1/2		3 3 2	14 1/2	14 1/2
0 5 2	16 1/2	− 14 1/2		3 4 2	15 1/2	15 1/2
0 6 2	15	15		3 6 2	5	4
0 7 2	15 1/2	15 1/2		3 8 2	8 1/2	8
0 9 2	4	3		3 9 2	10	− 9 1/2
0 11 2	8	6		3 10 2	9	− 9 1/2
0 12 2	9	− 7 1/2		4 0 2	7	8
0 13 2	8	− 7 1/2		4 1 2	6 1/2	7
1 0 2	5	− 4		4 5 2	5 1/2	5
1 2 2	10	− 9 1/2		4 6 2	6 1/2	− 6
1 3 2	10 1/2	9 1/2		4 7 2	6	− 6
1 4 2	10	9 1/2		5 2 2	6	− 4 1/2
1 6 2	2	2		5 3 2	5	4 1/2
1 8 2	5	4 1/2		5 4 2	6 1/2	5 1/2

hkl	F_{obs}	F_{calc}	hkl	F_{obs}	F_{calc}
6 0 2	8	9	2 12 3	11 1/2	−9 1/2
6 1 2	10	9	2 13 3	6	6
6 3 2	3	2 1/2	4 0 3	18	−18 1/2
6 5 2	5	6	4 1 3	8 1/2	11
6 6 2	8 1/2	−7	4 3 3	6 1/2	5 1/2
6 7 2	7 1/2	−7 1/2	4 5 3	7 1/2	8
7 3 2	3 1/2	−4	4 6 3	14	14
1 0 3	8	−9	4 7 3	7 1/2	−8 1/2
1 2 3	12	−14 1/2	4 9 3	3	−3
1 3 3	21	−25	4 11 3	3	−3 1/2
1 4 3	13	14 1/2	4 12 3	8	−7 1/2
1 6 3	7	6 1/2	5 0 3	6	6 1/2
1 8 3	7	8	5 2 3	6	9
1 9 3	13	15	5 3 3	14	16
1 10 3	8	−9	5 4 3	9	−9
1 12 3	1	−3	5 6 3	4	−4 1/2
2 0 3	24 1/2	−26	5 8 3	4	−4
2 1 3	14 1/2	14 1/2	5 9 3	10	−10
2 3 3	8	8	5 10 3	6	6
2 5 3	10	10 1/2	7 2 3	4	5
2 6 3	20	20	7 3 3	8 1/2	9
2 7 3	12	−12	7 4 3	5	−5
2 9 3	6	−5	8 0 3	9	9
2 11 3	4	−4 1/2	8 1 3	4 1/2	−5

hkl	F_{obs}	F_{calc}	hkl	F_{obs}	F_{calc}
0 0 4	13	−12	0 2 6	3	2
0 6 4	7	9	0 3 6	5 1/2	6 1/2
0 12 4	4	−4 1/2	0 4 6	3	−2
1 3 4	5	5 1/2	0 5 6	7	10 1/2
2 0 4	6 1/2	−5 1/2	0 6 6	3	2
2 6 4	4	4	0 7 6	10	−11
3 3 4	8	9	0 9 6	4 1/2	−4
3 9 4	5	−5 1/2	1 2 6	5	6
4 0 4	3 1/2	4 1/2	1 4 6	5 1/2	−6 1/2
1 2 5	4	−3 1/2	1 8 6	3	−3 1/2
1 3 5	17 1/2	19 1/2	1 10 6	4	4 1/2
1 4 5	4 1/2	4	2 1 6	5 1/2	6
1 9 5	13	−12	2 5 6	3 1/2	4 1/2
2 0 5	21	20	2 7 6	5	−5
2 1 5	5	3	3 0 6	7	6
2 6 5	16 1/2	−16	3 2 6	11 1/2	11
2 12 5	11	8 1/2	3 4 6	12	−11
4 0 5	15	15	3 6 6	4 1/2	−4 1/2
4 3 5	14	−2	3 8 6	6 1/2	−6 1/2
5 3 5	11	−13	3 10 6	8 1/2	8
5 9 5	11	9	6 1 6	6 1/2	−7 1/2
0 0 6	3 1/2	−2 1/2	0 0 8	12	11
0 1 6	11	14	0 1 8	3	−4

hkl			F_{obs}	F_{calc}
0	3	8	5	-4
1	3	8	6	$-5\ 1/2$
2	0	8	6	5
3	0	8	4 1/2	-4
3	3	8	10 1/2	$-9\ 1/2$

Biographical Note

Leonid Vladimirovitch Azaroff, son of Vladimir
I. Azaroff, Ph.D., and Maria Y. Azaroff, B.S., was born in
Moscow, Russia on June 19, 1926. He spent his early child-
hood in Riga, Latvia, where he obtained his elementary
education. In 1939, the Azaroff family emigrated to the
United States.

His secondary school education was completed
in the United States when he graduated from the Berkeley
Preparatory School, Boston, Massachusetts, in August, 1943.
In September of that year he was awarded a scholarship
at Tuft's College, and enrolled in the Physics Department
where he remained until called to enter the service in
1944.

During part of the two years spent in the service,
he attended the Virginia Polytechnic Institute, Blacksburg,
Va. where he studied civil engineering for three terms.
During the last year he was stationed at Fort Belvoir, Va.,
where he worked as a research assistant in the Infra-Red
Section of the Army Engineer Board. He was honorably dis-
charged in 1946.

Upon return to civilian life, he re-entered Tufts
College, from which he received a B.S., cum laude, in

Physics, in June, 1948. While attending Tufts College he was elected to $\Sigma \Pi \Sigma$, Physics Honorary Society and became a member of the American Association of Physics Teachers and the American Institute of Physics.

In September of 1948 he was admitted to the Graduate School of the Massachusetts Institute of Technology where he worked towards a Ph.D. in geophysics. In the summer of 1950, he attended a special summer course in x-ray crystallography at Brooklyn Polytechnic Institute, Brooklyn, N.Y., and upon returning to M.I.T. in the fall changed his major field to crystallography. He held an appointment as teaching fellow in 1952 and 1953 during which time he assisted in the teaching of Elementary Crystallography, Theoretical Crystallography and X-Ray Mineralogy. From September, 1952 to June, 1953 he was appointed a full-time research assistant and conducted research in crystallography. In 1952 he was elected to ΣX, Graduate Honor Society. He is also a member of the American Crystallographic Association and the Mineralogical Society of America. He presented a paper titled "A One-Dimensional Analogue Computer" at the June, 1953 meeting of the A.C.A. and has published an article titled "A Telescoping Direct-Beam Tunnel" in the <u>Review of Scientific Instruments</u>. (1953)